The Origin of Systematic Errors in GCM Simulations

of ITCZ Precipitation over the Ocean

Winston C. Chao[1], Max J. Suarez[1*], Julio T. Bacmeister[2*],

Baode Chen[3, 4*] and Lawrence L. Takacs[3*]

1 NASA/Goddard Space Flight Center, Greenbelt, MD 20771

2 Goddard Earth Sciences and Technology Center, University of Maryland, Baltimore County, Baltimore, MD 21250

3 Science Applications International Corporation, Lanham, MD 20706

4 Presently with the Shanghai Meteorological Bureau, Shanghai, China 200030

* Goddard Modeling and Assimilation Office, NASA/Goddard

Corresponding Author Address:
Dr. Winston C. Chao
Mail Code 613.2
NASA/GSFC
Greenbelt, MD 20771

Winston.c.chao@nasa.gov

Abstract

This study provides additional explanations for some of the experimental findings of Chao (2000) and Chao and Chen (2001, 2004) concerning the mechanisms responsible for the latitudinal location of the ITCZ (intertropical convergence zone) in an aqua-planet model. These explanations are given in terms of attractors that are caused by the earth's rotation and sea surface temperature (SST) latitudinal distribution. These explanations are then used to explain the origin of some of the systematic errors in the GCM (general circulation model) simulation of ITCZ precipitation over the ocean, including the origin of the "double-ITCZ bias."

When the influence of the SST distribution is excluded, the earth's rotation, by itself, can generate either a single rotational ITCZ attractor at the equator or a double rotational ITCZ attractor at approximately 15° N&S, depending on the model physics. When a double rotational ITCZ attractor is generated, if it is excessively strong due to problems with the model physics, the addition of the attraction due to the SST distribution will not be able to turn a double ITCZ into a single ITCZ in the non-equinoctial seasons. This results in a "double-ITCZ bias," with the component of the double ITCZ on the opposite side of equator from the SST latitudinal peak being stronger than the component on the same side of the equator as the SST latitudinal peak. On the other hand, when a single rotational ITCZ attractor over the equator is generated, a single ITCZ exists between the equator and the SST latitudinal peak (assuming there is only one SST latitudinal peak), which is too close to the equator year-round. In fact, to obtain a

good ITCZ simulation, the model should have a double rotational ITCZ attractor of moderate strength.

ITCZ precipitation systematic errors are highly sensitive to the model physics, and by extension, the model horizontal resolution. A few possible methods of alleviating systematic errors in the GCM simulation of the ITCZ precipitation--such as rain re-evaporation, cumulus momentum transport, and an extra condition on the cumulus parameterization scheme--are discussed in the context of experiments using a recent version of the Goddard Modeling and Assimilation Office's Goddard Earth Observing System (GEOS-5) GCM. One of the important findings is that the ITCZ precipitation systematic-error problem should be studied in conjunction with other problems in the GCM simulation, such as the problem in simulating the tropical wavenumber-frequency power spectrum.

The contribution of this paper is mainly conceptual. This paper's findings, along with those of Chao (2000) and Chao and Chen (2001, 2004), contribute to building a theoretical foundation for ITCZ study that may lead to the eventual diminution of ITCZ precipitation systematic errors in GCMs.

1. Introduction

The latent heat released in the intertropical convergence zone (ITCZ) drives (or, more precisely, interacts with) the Hadley/Walker circulation; thus, how well the location and intensity of the ITCZ precipitation are simulated in a general circulation model (GCM) is a fundamental factor in the performance of a GCM. In fact, most GCMs have large systematic errors in the location and intensity of the ITCZ precipitation. In some GCMs, the ITCZ precipitation in the western and central Pacific in the June-July-August (JJA) season--when the SST peak is in the northern hemisphere--can be so unrealistic as to have a local maximum in the southern--the incorrect—hemisphere. This is true for the NCAR CCM3, as shown in Fig. 22 of Hack et al. 1998; for an earlier version of the NASA seasonal-to-interannual prediction project (NSIPP) model (Fig. 1 of Bacmeister et al. 2006); and for the NCAR CCSM3 (Fig. 1a of Zhang and Wang 2006). Besides having a local ITCZ precipitation maximum in the southern—the wrong—hemisphere in the JJA season, these models also have another weaker local ITCZ precipitation maximum on the other side of the equator; thus they have a distinct "double-ITCZ bias." The double-ITCZ bias occurs not only in coupled ocean-atmosphere GCMs (more recent references are Lin 2007 and De Szoeke and Xie 2008) but also in atmospheric GCMs with specified SST. The wrong-hemisphere problem may also exist in the western and central Pacific in the Dec-Jan-Feb (DJF) season (e.g., Fig. 21 of Hack et al. 1998).

A related question is why the GCM-simulated local ITCZ precipitation maximum does not appear in the wrong hemisphere in the eastern Pacific or in the Atlantic in the JJA season. Most GCMs, after some empirical modifications, are not so incorrect as to

have their local ITCZ precipitation maxima in the wrong hemisphere, but they still have the lesser problem of incorrect ITCZ precipitation intensity. Why empirical modifications have helped remove the wrong-hemisphere problem and how the intensity problem can be resolved are additional questions.

Another common problem in GCMs is a reduction in the ITCZ precipitation in the middle of the northeastern Pacific: i.e., the precipitation tends to be concentrated in the coastal region next to Central America, where there is a local SST maximum (e.g., Fig. 22 of Hack et al. 1998). Some models also exhibit a high concentration of ITCZ precipitation over the local SST maximum in the equatorial western Atlantic. Moreover, in some models, the ITCZ precipitation peak in the Indian Ocean may be located too close to the equator in the JJA season. Examples of these problems will be presented in section 5.

Though systematic errors in ITCZ precipitation are by no means the only errors in GCMs, they have been conspicuous and well-known ever since the beginning of GCM modeling research. Correcting these errors is an important area of study that has attracted many researchers (e.g., Wu et al. 2003, Bacmeister et al. 2006, and Zhang and Wang 2006). So far, this pursuit has been based on empirical trial-and-error approaches, and progress has been very limited. Understanding the causes of these systematic errors would greatly aid in correcting them. Hence, the purpose of this paper is to examine how these systematic errors arise in an attempt to contribute to the larger goal of building a theoretical foundation for ITCZ study.

The previous theoretical and modeling studies of the ITCZ by Chao (2000) and Chao and Chen (2001, 2004) using an aqua-planet model provide a starting point for our

study here. We will briefly review these aqua-planet ITCZ studies in section 2, and in section 3—the core part of this article, apply the knowledge reviewed in section 2 to explain conceptually the cause of systematic errors in GCM ITCZ precipitation simulation over the ocean. Some possible methods to correct these errors will be discussed in section 4. In section 5, we will support our explanations given in section 3 with GCM experiments using a recent version of the Goddard Earth Observing System (GEOS-5) GCM. These experiments also include some done with an aqua-planet version of the GEOS GCM with zonally-uniform SST, which show nonlinear nature of the sensitivities of the ITCZ location to changes in model physics.

The basic intent of the experiments presented in section 5 is not to correct ITCZ systematic errors (location and intensity) in GCMs, but to support the explanation in section 3 of how ITCZ systematic errors can arise. Much more than what we present in this article has to be done, both conceptually and experimentally, before the ITCZ systematic errors can be corrected. The scope of this paper is only to provide the conceptual explanation for how ITCZ systematic errors can arise and hopefully this explanation can be useful in the future effort of correcting ITCZ systematic errors. Also, atmosphere-ocean interaction is not discussed in this paper. Interested readers are referred to existing literature on that topic (e.g., Philander 1996, de Szoeke et. al 2006.) We will conclude with a summary and remarks in section 6.

2. A brief review of the fundamental mechanisms governing the ITCZ's latitudinal location in aqua-planet settings

To proceed with our study, we need to delve into the fundamental physical mechanisms that are responsible for the ITCZ. These mechanisms are most clearly revealed in aqua-planet (AP) GCM simulations with zonally-uniform sea surface temperature (SST), since these AP GCMs provide simplified settings to examine the ITCZ (e.g., Sumi 1992, Hess et al. 1993, Kirtman and Schneider 2000, Chao 2000, Chao and Chen 2001, 2004). Under these settings, the latitudinal location of the ITCZ is determined by the earth's rotation, the interaction among model physics components, and the SST latitudinal profile. An even more simplified AP model setting is one without horizontal and temporal variations in SST and solar angle. This case will be reviewed first. The case of SST varying only in the latitudinal direction will be reviewed subsequently. The reader is reminded that this section is only a brief review; for a detailed description the reader is referred to Chao (2000) and Chao and Chen (2001, 2004).

Before presenting the details of the review it is useful to summarize the mechanisms that determine the latitudinal location of the ITCZ. The latitudinal location of the ITCZ in an aqua-planet setting is determined by the balance of forcings on the ITCZ. There are basically two types of forcings on the ITCZ, which push the ITCZ in the latitudinal direction. One type of forcing is due to the earth's rotation, denoted by R, which exists even when the SST and solar angle are globally uniform. The other type of forcing is due to the SST latitudinal peak solely without the presence of the earth's rotation, denoted by S, assuming that the SST is zonally symmetric and its latitudinal profile is Gaussian. R can be further broken down into two components. (Note that the word "forcing" is used instead of "force". This is because the ITCZ is a flow pattern not

an object with mass. "Force" has the meaning of *mass* multiplied by acceleration. Also, we use the words "forcing" and "attraction" interchangeably.)

2a. *Aqua-planet model with globally- and temporally-uniform SST and solar angle*

A study of the ITCZ in an AP model with globally- and temporally-uniform SST and solar angle by Chao and Chen (2004) showed that the ITCZ under such settings could be either a single ITCZ over the equator or a double ITCZ at approximately 15°N&S, depending on the model physics. Sometimes only one component of the double ITCZ appears,[1] resulting in a single ITCZ *away* from the equator—which is distinctly different from a single ITCZ *over* the equator. Whether a single or a double ITCZ appears is determined by the earth's rotation, the interaction between convection and surface fluxes through the earth's rotation, and the interaction between convection and radiation. Since convection is central to these interactions, the cumulus parameterization scheme plays a very important role in GCM simulation of the ITCZ.

Chao and Chen (2001) performed some experiments in which the relaxed Arakawa-Schubert scheme (RAS, Moorthi and Suarez 1992) was allowed to operate only when the boundary-layer relative humidity rose above a certain critical value. By increasing this critical value, the behavior of the cumulus parameterization scheme could be changed from that of RAS to that of the moist convective adjustment scheme (MCA, Manabe et al. 1965), and the ITCZ could be correspondingly changed from a double ITCZ to a single ITCZ over the equator.

[1] This remains a puzzle; others have encountered the same phenomenon in different models with uniform SST (e.g., Pike 1971, Raymond 2000, Barsugli et al. 2005.)

Chao and Chen (2004) hypothesized that under globally- and temporally-uniform SST and solar angle conditions, the ITCZ experiences two opposing types of attraction--both due to the earth's rotation--and that the latitude where these two attractions balance each other is where the ITCZ resides. The first type of attraction is due to inertial stability, which pulls the ITCZ (or, more precisely, the individual synoptic-scale convective systems that compose the ITCZ) toward the equator (see section 3 of Chao and Chen (2001) for an explanation). This type of attraction does not depend on the model physics. The second type of attraction (also on the individual synoptic-scale convective systems that compose the ITCZ) is due to the latitudinal gradient of the Coriolis parameter-modified surface heat fluxes that are associated with synoptic convective systems, which pulls the ITCZ toward one of the poles (see the discussion in Chao and Chen 2004 that is related to its Fig. 11 for an explanation). The degree of modification of the surface heat fluxes by the Coriolis parameter depends on the cumulus parameterization scheme, as well as on other components of the model physics.

The magnitudes of these two types of attraction on the ITCZ as functions of the latitude of the ITCZ are depicted schematically in Fig. 15 of Chao and Chen (2004), which is reproduced here as Fig. 1. Using the argument that convection occur at the latitude when the inertio-gravity waves are most unstable, i.e., the latitude where the squared frequency of the gravity waves, $\omega^2 = f^2 + \alpha^2 N^2 + |F|$ (Eq. 8.4.23 of Gill 1982), has a minimum (i.e., the latitude where $\partial\omega^2/\partial\phi=0$, where ω^2 is expected to be negative, since convection is expected to occur somewhere over the globe, given the radiative cooling and surface heat fluxes, which make the atmosphere convectively unstable), where f is the Coriolis parameter, α the ratio of the vertical scale to the horizontal scale

of the synoptic-scale connective system, N^2 the vertical stability, and |F| the frictional term; Chao and Chen (2004) quantified the two attractions as the two latitudinal gradients $\partial f^2/\partial\phi$ and $\partial(-\alpha^2N^2 - |F|)/\partial\phi$. The magnitude of the first type of attraction—represented by curve A (a positive value means southward attraction)—can be determined analytically and is equal to the $\partial f^2/\partial\phi$, i.e., $8\Omega^2 \sin\phi \cos\phi$ (in the units of s^{-2}), with f being the Coriolis parameter, Ω the earth's rotation rate, and ϕ the latitude. The magnitude of the second type of attraction—represented by curve B (a positive value means northward attraction)—cannot be determined analytically and must be determined experimentally. Curve B is the latitudinal gradient of $-(\alpha^2N^2)$. N^2 is a function of vertical profiles of temperature and moisture, which are related to the surface heat fluxes; the latter in turn are related to the surface winds and the surface winds are related to the Coriolis parameter. The latitudinal gradient of |F| can be incorporated into curve B. See Chao and Chen (2004) for details. Naturally, there can be secondary instability that can affect ITCZ location and structure (see Appendix C), but it is important to grasp that the primary reason the ITCZ exists is convective instability.

Chao and Chen (2004) postulated that the conditions for MCA to operate are more restrictive than for RAS, and therefore under MCA, the modeled synoptic convective systems are more vigorous, and thus the associated surface wind--and in turn, surface fluxes--are less affected by the earth's rotation. This is because in a model using MCA, after an air parcel moves down into the boundary layer, it moves quickly toward the center of the convective system and spends a very short time being affected by the Coriolis force to increase its speed. As a result, in Fig. 1, curve B_{MCA} is smaller than curve B_{RAS}.

For RAS, the stable balance between the two types of attraction, denoted by point P in Fig. 1, is at approximately 17°N&S, and for MCA, the stable balance is at the equator. (These locations are called the rotational ITCZ attractors (Chao and Chen 2001.) By attractor[2] we simply mean the location toward which the attraction forcing is directed; no connotation is attached to it.) Therefore, RAS yields a double ITCZ straddling the equator, whereas MCA yields a single ITCZ over the equator. The net attraction on the ITCZ (a positive value means southward attraction) is depicted as curve R (where R=A-B) in Figs. 2a and 2b for RAS and MCA, respectively (reproduced from Chao (2000).

When a condition is added to RAS such that the boundary-layer relative humidity must be above a certain critical value, the condition for RAS to operate becomes stricter and RAS behaves more like MCA--i.e., in Fig.1, B_{RAS} is reduced to B_{MCA} as this critical value, RHc, is increased. As a result, a double ITCZ turns into a single ITCZ.

Chao and Chen (2004) pointed out that the failure of earlier ITCZ theories to explain the ITCZ latitudinal location in AP models with globally- and temporally–uniform SST and solar angle was due to the invalidity of CISK and wave-CISK theories, upon which the earlier theories were built, and to not recognizing the existence of curve B in Fig. 1.

---

[2] We use the word attractor in the following sense. When there is a forcing pushing the cloud cluster towards a certain latitude (e.g., equator, poles, or any other latitude), we say that certain latitude is the center of the attractor. All the attractors we discussed have global scale. For example, curve A represents the forcing that a cloud cluster experience because of the inertial stability which pushes it toward the equator. In this case the equator is the center of the attractor. In other words, if the inertial stability were the only mechanism existing, a cloud cluster located away from the equator would move toward the equator (the center of the attractor) because at the equator the inertial stability is the least—i.e., nonexistent. Thus, we can say that the cloud cluster experiences a forcing due to inertial stability and we represent the magnitude of this forcing as a function of the latitude of the ITCZ by curve A.

It is noted that Fig. 6 of Chao and Chen (2001) and its associated explanation of RN and RS are now considered as too vague and they have been superseded by Fig. 15 of CC04, which is Fig. 1 of this paper, and its associated explanation.

2b. *Aqua-planet model with an SST latitudinally-varying profile*

When the SST distribution is changed from globally-uniform to latitudinally-varying (but is still zonally-uniform) and is given a Gaussian-shape latitudinal dependence, the ITCZ experiences an additional type of attraction toward a latitude offset slightly poleward from the SST peak. This is shown in Fig. 11 of Chao (2000), in an experiment without the earth's rotation. In this experiment, as the SST peak is moved poleward--with the shape of the SST latitudinal Gaussian profile remaining unchanged--the ITCZ offset from the SST peak increases.[3] But this offset remains small. This new type of attraction is depicted in Figs. 2a and 2b as line S. Chao (2000) provided an explanation as to why this attraction could be approximately represented as a straight line. The explanation is that since the SST latitudinal Gaussian profile has a global scale the attractor that it generates (with the center of the attractor at the latitude of the SST peak) must have a global scale as well. Thus, the corresponding attraction can be approximately represented by a linear line in the limited domain close to the center of the

[3] The explanation for the poleward offset of the ITCZ from the SST peak is as follows: When the SST peak is at the equator in this experiment, the equator is the latitude of symmetry and the ITCZ is located there; but when the SST peak is moved away from the equator, the earth's geometry is no longer symmetric with respect to the SST peak. Then, the poleward side of the SST peak has a higher averaged SST, and thus the ITCZ is located slightly poleward of the SST peak. The degree of asymmetry, and thus the size of the offset, becomes larger as the SST peak is moved farther away from the equator.

attractor—i.e., the tropics. Obviously, the slope of line S (or how close it is to being vertical) is an indication of the strength of the attraction due to the SST peak.

When both the earth's rotation and a Gaussian SST latitudinal profile exist within an experiment, the balance in Fig. 2 between curve R (a positive value means southward attraction), representing the rotational forcing (i.e., the difference between curves A and B in Fig. 1), and line S (a positive value means northward attraction) determines the latitudinal location of the ITCZ for both RAS and MCA. Thus, the ITCZ is located at the latitude where the net forcing, R-S, is zero. If RAS is used and the SST peak remains at the equator and becomes sharper--i.e., if line S becomes more vertical--the two components of the double ITCZ draw closer together and eventually merge. (See Fig. 13 of Chao (2000) for the result of such an experiment.) The speed of this merger is quite slow due to the fact that in Fig. 2b at the moment the double ITCZ cease to exist, as the slope of line S is increased slowly, curve R and line S almost coincide with each other between 10S and 10N and thus the net forcing (R-S) on the ITCZ is almost zero.

If the SST Gaussian latitudinal profile retains its shape but is moved latitudinally, the ITCZ structure can change quite dramatically. Figs. 10 and 11 of Chao and Chen (2001) show the results of such an experiment for the RAS and MCA types of convection schemes, respectively. When MCA is used and the SST peak is moved northward from the equator, consistent with Fig. 2a, a single ITCZ follows behind the SST peak and then suddenly starts to catch up, but does not quite reach the SST peak; thereafter, the ITCZ appears to be almost stationary despite further northward movement of the SST peak. When RAS is used, there are two latitudes where curve R and line S are in stable balance if the SST peak is not too far away from the equator (Fig. 2b). Thus, there is a double

ITCZ. As the SST peak is moved northward from the equator, both ITCZ components move northward, and the southern component of the double ITCZ becomes stronger than the northern component. Finally, the southern component of the double ITCZ moves rapidly to merge with the northern component, and thereafter, the merged single ITCZ remains almost stationary despite further northward movement of the SST peak. This phenomenon, shown in Fig. 3 of Chao and Chen (2001), has not been previously explained. The explanation for this phenomenon is a prerequisite for our answers to the theoretical questions posed in the introduction and will be given in section 3.

2c. *Remarks*

Our interpretation of the AP experimental results does not require that the combined effect of the rotational attraction and the SST peak attraction on the ITCZ be equal to a simple addition of the two individual attractions. See Appendix B for a discussion of this non-additive assumption. Also, some discussion on Fig. 1 about the sudden movement to the equator when RHc is increased is given in Appendix C.

Also, when applying the concepts in this section to the full GCM, one needs to allow the SST slope to take on different values in different geographical locations.

3. Explanation for systematic errors in the GCM simulation of ITCZ precipitation over the ocean

3a. *Explanation for the behavior of the ITCZ in responding to latitudinal movement of the SST peak*

The explanation for the ITCZ's behavior illustrated in Fig. 3 of Chao and Chen (2001) is as follows. There is a nearly-vertical demarcation line in the zonal mean meridional circulation separating the northern components of the meridional circulation cells from the southern components. One may call the latitude of this demarcation line the "meridional circulation equator" (or, "circulation equator" for the sake of brevity). When the SST peak is at the equator, the circulation equator is there too. When the SST peak is moved northward from the equator, the circulation equator--which lies midway between the two double ITCZ components that are moving northward--should move northward as well. As the circulation equator moves north of the equator, the tropical area south of the circulation equator becomes larger than the tropical area north of it. Since the latent heat released in the southern component of the double ITCZ is now responsible for balancing the radiative cooling of a larger area, the southern component of the double ITCZ should become stronger than the northern component.[4] Thus, as the SST peak is moved north from the equator, the southern component of the double ITCZ strengthens. As the SST peak is moved farther north of the equator, its attraction no longer balances the two rotational attractors separately. Now, in Fig. 2b, line S no longer intersects curve R south of the equator--i.e., the attraction due to the SST peak has to deal with the two rotational attractors as a whole. Therefore, the double ITCZ now becomes a

[4]Although the ITCZ is not responsible for all the convective heating, it is by far the main contributor. Also, there can be net energy flux across the MCE; but since the Hadley circulation is dominant in the tropics, this flux is negligible.

single ITCZ--i.e., the southern component of the double ITCZ moves rapidly to merge with the northern component.

3b. *Explanation for how the simulated ITCZ precipitation maximum can be in the wrong hemisphere (the source of the double-ITCZ bias)*

In Fig. 2b (taken from Chao 2000), it is obvious that if the slope of line S becomes greater (i.e., if line S becomes more vertical) relative to curve R through a modification of the model physics, the two components of the double ITCZ will merge sooner (i.e., the southern ITCZ will move to merge with the northern ITCZ sooner) as the SST peak is moved north of the equator. Conversely, if the slope of line S relative to curve R is not great enough, or if the SST peak is not moved far enough from the equator, the merger will not happen. For a seasonal movement of the SST peak that moves only between, e.g., 5°S and 10°N (as does the observed SST peak in the Pacific, ignoring the minor peak northeast of Australia; or as does the observed zonal mean SST), a lesser slope of line S relative to curve R--by not allowing the merger to occur--yields a seasonal cycle of a double ITCZ year-round with a stronger southern component in the JJA season—i.e., a double-ITCZ bias. Moreover, a steeper slope of line S relative to curve R yields a double ITCZ structure only in off-JJA seasons and yields a single northern ITCZ in the JJA season, the latter when the SST peak is farthest north of the equator. Note that there are two types of double ITCZ bias. The first type is that the model shows a double ITCZ in a region(s), but the corresponding observation shows only a single ITCZ. The second type is that the model shows too strong a double ITCZ, but the corresponding

observation shows a weak one. Our work deals with type 1 double ITCZ bias only. The mere existence of a double ITCZ in a model does not mean a double ITCZ bias of the first type has occurred; the double ITCZ has to exist when the real, or the expected, situation is a single ITCZ to be labeled as a double ITCZ bias of the first type. Type II double ITCZ bias is not as severe as type 1 and thus far has not been given much priority, but it should be attended to in the future.

No double-ITCZ bias occurs in the eastern Pacific in the JJA season because the SST there has a much stronger meridional peak (i.e., line S has a steeper slope relative to curve R) than in the central and western Pacific (where a double-ITCZ bias can occur). This strong SST meridional peak is a result of the equatorial SST minimum in this region. Also, the fact that this SST meridional peak is located away from the equator in the northern hemisphere (Figs. 4e and 4f) also minimizes the likelihood of double ITCZ in this region in JJA. A GCM has to have severely wrong model physics so that curve R sits beyond the dotted curve in Fig. 2c to generate double-ITCZ problem in this region in JJA.

3c. *Explanation for how the simulated ITCZ precipitation maximum can remain at an equatorial location year-round*

From Fig. 1, it is seen that by changing the cumulus parameterization scheme gradually (e.g., as discussed in Chao and Chen (2004) in association with their Figs. 2 and 3), curve R can be gradually changed from the shape shown in Fig. 2a to the shape shown in Fig. 2b. In between, curve R--relative to line S--can take on different shapes, as

shown in Fig. 2c. For those R curves that have substantially-positive R-minus-S values just north of the equator, there is a stable intersection point between curve R and line S at an equatorial location, and if the SST peak is not moved far enough away from the equator, the ITCZ can remain at or near the equator year-round.

3d. *Remarks*

Curve R--relative to line S--in Fig. 2 can be changed as a result of changing curve B in Fig. 1, through changes in the model physics. Different R curves (Fig. 2c), relative to line S, give rise to different systematic errors, which can fall between the two types described in subsection 3b and 3c. Because of regional SST distribution differences, curve R--relative to line S--can be somewhat different in different geographical regions both in GCMs and in nature. To minimize systematic errors in simulating the ITCZ over the ocean, curve R--relative to line S--should approximate the solid curve in Fig. 2c, which represents the situation in nature. If curve R deviates sufficiently toward the dotted line in Fig. 2c, a double-ITCZ bias arises, and if it deviates sufficiently in the other direction, the ITCZ remains too close to the equator year-round. Finally, as a reminder, our present study is based on concepts proposed for an aqua-planet model with a single SST peak. Hence, our ideas may not be applicable to regions over or close to a landmass, or to regions where there are two latitudinal SST peaks.

4. Some possible methods of correcting ITCZ systematic errors over the ocean

For a GCM that has local ITCZ precipitation maxima in the southern hemisphere in the central and western Pacific in the JJA season, one should be able to correct this problem by sharpening the SST peak in the northern hemisphere in the JJA season or by changing the model physics such that line S becomes more vertical relative to curve R in Fig. 2b. Or, if a model has its ITCZ precipitation maxima over or too close to the equator in a region when they are not supposed to be, one should try to change the model physics such that curve R--relative to line S--becomes more like the solid curve in Fig. 2c. Of course, changing the SST peak, as suggested above, is not a real option, but it can verify our idea.

The next question is how to change the model physics. We will discuss three possibilities. As demonstrated in Chao and Chen (2004), curve B in Fig. 1--and therefore curve R in Fig. 2--can be changed by changing the cumulus parameterization scheme. One way to do this, as Chao and Chen (2004) suggested, is to add a condition to the cumulus parameterization scheme such that it is allowed to operate only when the boundary-layer relative humidity exceeds a certain critical value, RHc. As this critical value is increased, convection is less apt to occur, but when it does occur, it is more vigorous. A more vigorous convection scheme correlates with a reduction in the magnitude of curve B, as explained in subsection 2a. Thus, as the critical value RHc is increased, the magnitude of curve B is reduced.

Curve A (Fig. 1) is not changed by changing the model physics, such as by changing the cumulus parameterization scheme. Therefore, as the magnitude of curve B is reduced, curve R changes in the direction from the dotted curve to the long-dashed curve in Fig. 2c, since R=A-B, as explained in subsection 2a. Of course, changing RHc

also affects the slope of line S. However, this slope must remain negative, since the equator remains the center of an SST attractor. In contrast, changing RHc can change curve R so drastically as to change its sign. Hence, relative to the change in curve R, the change in the slope of line S as result of changing RHc is relatively minor. The net effect of increasing RHc is to change curve R, relative to line S, in Fig. 2c in the direction from the dotted curve toward the long-dashed curve.

A second possible change in the model physics is to change the rate of re-evaporation of the cumulus rainfall. With rain re-evaporation intensified--which reduces the net convective heating--synoptic-scale convective systems are less vigorous. But exactly how curve R and line S are changed by adding rain re-evaporation requires further study. Whether rain re-evaporation should be increased or decreased so as to realize its beneficial effect will have to be determined by experimentation.

A third possible change in the model physics is to modify the cumulus momentum transport (CMT). Intensifying the CMT reduces the intensity of synoptic-scale convective systems and should have similar--but not identical--effects as intensifying rain re-evaporation.

Increasing the horizontal resolution tends to make cumulus convection more concentrated--i.e., making the horizontal scale of convective systems smaller. (This is due to the unfortunate fact that resolution-dependent physical parameterization schemes have not yet been developed. In other words, changing horizontal resolution effectively changes physical parameterization schemes.) Since, as mentioned in subsection 2a, curve B in Fig. 1 is inversely related to the square of the horizontal scale of the convective circulation, increasing horizontal resolution decreases the horizontal size of the

convective systems that make up the ITCZ and therefore increases α and thus the magnitude of curve B in Fig. 1. This, in turn, has the effect of moving curve R in Fig. 2c in the direction from the long-dashed curve toward the dotted curve, as described in subsection 3c. Changing curve R from the long-dashed curve to the dotted curve corresponds to changing a single ITCZ over the equator to a double ITCZ straddling the equator. This is consistent with Sumi's (1992) finding that, in an aqua-planet model with uniform SST and horizontally-uniform net radiative heating, increasing the horizontal resolution turned a single ITCZ over the equator into a double ITCZ straddling the equator.

The fact that the ITCZ can change from a single ITCZ over the equator to a double ITCZ straddling the equator is an example of why GCMs behave very differently and require re-tuning when the horizontal resolution is changed. The undesirable situation of model results having a regime change when the horizontal resolution is changed is a consequence of current cumulus parameterization having not taken into account the resolution-dependence. In the future, when resolution-dependent physical parameterization schemes are developed, this kind of model behavior should cease. See Jung and Arakawa (2004) for a further discussion on resolution-dependent physical parameterizations. The effects of changing vertical resolution remain to be explored.

Of course, there can be many other ways of modifying the model physics to change curve R relative to line S in Fig. 2c and thus correct systematic errors in ITCZ precipitation over the ocean. The mechanisms of how such modifications might effect their changes remain to be investigated. Also, for the three possible ways of changing the model physics that we have just discussed, each may have its own side-effects. For

example, intensifying rain re-evaporation may yield excessive relative humidity at low levels. Thus, the final solution to correcting systematic errors in GCM simulations of ITCZ precipitation over the ocean will have to be a combination of several modifications of the model physics. This point will be expanded in section 6.

In the next section, we will present some supporting GCM experiments on the model physics changes discussed in this section.

5. Supporting experiments

The model used for this study was a recent version of the Goddard Modeling and Assimilation Office's (GMAO) Earth Observing System (GEOS-5) GCM. The model has the finite-volume dynamical core of Lin (2004), the combined boundary-layer and turbulence package of Louis (1979) and Lock et al. (2000), the land-surface model of Koster and Suarez (1996), the radiation package of Chou and Suarez (1994, 1999), the relaxed Arakawa-Schubert scheme (RAS, Moorthi and Suarez 1992), and the prognostic cloud scheme and the rain re-evaporation scheme of Bacmeister et al. (2006). The cumulus momentum transport scheme advects momentum using the cumulus mass flux calculated in RAS. The resolution we used was 2.5° (lon), 2° (lat), and 32 levels. We created an aqua-planet version of the GEOS-5 model and used it and the full model for our experiments.

5a. Aqua-planet model experiments

We did ten one-year experiments with the AP model. In each experiment, the rain re-evaporation scheme was multiplied by a factor of EV and the cumulus momentum transport scheme was multiplied by a factor of CF. EV varied from 0 to 2, where 0 means rain re-evaporation was *not* used, 1 means rain re-evaporation *was* used, and 2 means the original rain re-evaporation intensity was doubled. CF was either 1 or 0--i.e., cumulus momentum transport was either used or not used (see Table 1).

In all these experiments, the initial condition was the end result of a three-year AP experiment with globally- and temporally-uniform SST (29°C) and solar angle Z (cosZ=0.25), starting from a resting atmosphere with minute perturbations in bottom-level winds, uniform surface pressure, and temperature and moisture fields as functions of height only. This initial condition was given a date of January 1, and had a double ITCZ. Also, the SST was a linear combination of 25% of a constant 29°C and 75% of a Gaussian latitudinal profile centered at the equator, as specified in Chao (2000, see its Eq. 1). In all ten AP experiments, the SST remained unchanged in the first 4 months. Then the SST latitudinal profile, while retaining its shape, was moved northward at a steady rate, by 15 degrees over 8 months.

Figs. 3a and 3b exemplify the results from the AP experiments. They show the zonally-averaged precipitation rate as a function of latitude and time for AE0.5C0 and AE0.75C1 (A for aqua-planet mode, E for EV and C for CF), respectively. Fig. 3a shows that as the SST peak is moved poleward from the equator, the single ITCZ behaves just like that in Fig. 2a—falling behind the SST peak at first and then catching up with it, but failing to do so completely, and then remaining almost stationary in spite of further poleward movement of the SST peak. This is essentially a repeat of the experiment

described in Fig. 2 of Chao (2000). Fig. 3b exhibits a double ITCZ in the first four months; after that, the southern component becomes stronger than the northern component as both components move northward. Eventually, the southern component crosses the equator to merge with the northern component. This is essentially a repeat of the experiment described in Fig. 3b of Chao and Chen (2001).

Table 1 summarizes the results of the ten aqua-planet model experiments for the period from May 1st to the end of the experiments (Dec. 31st). It shows that the results fall into three categories: 1) experiments that yielded a single ITCZ (designated by "single"); 2) experiments that yielded a double ITCZ where the southern component never crossed the equator (designated by "double"); and 3) experiments that yielded a double ITCZ where the southern component crossed the equator (designated by the month during which the southern component crossed the equator).

The change from a single ITCZ in AE0.5C0 to a double ITCZ in AE0.75C0 at the end of the first four months indicates that curve R in Fig. 2b has a small magnitude in AE0.5C0, so that it intersects line S only at the equator, but it has a larger magnitude in AE0.75C0, so that it intersects line S at three places, the outer two of them stable. In AE0.75C0 through AE2.5C0 (all with CF=0) (see Table 1), at the end of the first four months when the SST peak is still at the equator, a double ITCZ exists but the two components of the double ITCZ diverge more greatly with higher rates of rain re-evaporation. These results show that as the rate of rain re-evaporation is increased from AE0.5C0 to AE1.5C0, curve R, relative to line S, moves in the direction from the long-dashed curve in Fig. 2c towards the dotted curve.

In AE0.75C0 through AE1.5C0, as the SST peak is moved northward, the southern component of the double ITCZ intensifies and crosses into to the northern hemisphere later as the rain re-evaporation rate is increased. This corresponds to a decrease in the slope of line S relative to curve R in Fig. 2b, which is equivalent to changing R in the direction from the long-dashed curve toward the dotted curve in Fig. 2c while keeping line S unchanged. However, delaying the equator-crossing of the southern component of the ITCZ by increasing rain re-evaporation rate can worsen the double-ITCZ bias. This is contrary to the beneficial effect of rain re-evaporation found in the NSIPP model by Bacmeister et al. (2006). We will see later that when the horizontal resolution of our model is doubled, the beneficial effect of rain re-evaporation is realized.

Table 1 shows that inclusion of cumulus momentum transport can delay the equator-crossing of the southern component of the double ITCZ--i.e., by decreasing the slope of line S relative to curve R in Fig. 2b for EV=0.7 and EV=1.0. However, for EV>1, the delaying effect of adding cumulus momentum transport is reversed. Also, when cumulus momentum transport is included, a further increase in EV above 1 does not delay the merger of the southern component of the double ITCZ with the northern component. This indicates that curve R and line S in Fig. 2b increase at a rate to balance each other.

In summary, these AP model experiments demonstrate the highly nonlinear response of ITCZ behavior to changes in rain re-evaporation rate and cumulus momentum transport. They also illustrate the complexity of correcting ITCZ systematic errors.

5b. Full-model experiments

We also did four experiments with the full model at 2.5° (lon) by 2° (lat) and 72 levels of resolution--which is more than double the vertical resolution in both the troposphere and the stratosphere that was used in the AP experiments. The first two experiments, respectively, were FME1 with no rain re-evaporation (EV=0) and FME2 *with* rain re-evaporation (EV=1). The third experiment, FME3, was a repeat of FME1, but with a perturbation added to the observed SST used in FME1 in the JJA season. This perturbation took the form of a linear function of latitude from zero at the equator to 4°C at 20ºN, and another linear function of latitude from 4°C at 20ºN to zero at 40ºN. The fourth experiment, FME4, was a repeat of FME2 with a condition on RAS that the boundary-layer relative humidity had to be greater than 95%. In all four experiments, CF was set to 1.

The full-model experiments started from Oct 30, 1992, using the observed SST. Each ran for two years. The precipitation maximum in the eastern half of the Indian Ocean in FME1 and FME2 in the JJA season in 1993 and 1994 failed to reach the Bay of Bengal and was controlled by a local SST maximum (Figs. 4a and 4b). In the western half of the Indian Ocean, the precipitation maximum was very close to the equator in both FME1 and FME2, contrary to observations (Figs. 4g and 4h from Xie and Arkin (1998) data). The cause of this equatorial location has been explained in subsection 3c. In the northern Indian Ocean, the weak JJA precipitation in FME1 persisted in FME2. In the DJF season, both FME1 and FME2 exhibited a similar problem of the ITCZ being too close to the equator in the Indian Ocean, with the exception of the DJF season of 1993-94

in FME1, where there was a double ITCZ in the eastern Indian Ocean (Figs. 4c, 4d, 5c and 5d). Thus, rain re-evaporation did little for the problem of the ITCZ being too close to the equator year-round in the Indian Ocean.

In the JJA season, from the eastern edge of the Indian Ocean to about 135°E, FME1 had an ITCZ precipitation maximum at the correct latitude of about 17°N, where the SST latitudinal peak was located (see Figs. 4e and 4f); in contrast, FME2 had an ITCZ precipitation maximum in the correct hemisphere, but somewhat closer to the equator than seen in observations. From 135°E to 160°E, the ITCZ precipitation peak was almost exactly over the equator, and again coincided with the SST latitudinal peak in both FME1 and FME2. From 160°E to 130°W, both FME1 and FME2 had a double ITCZ, with the southern component (i.e., the SPCZ, or the southern Pacific convergence zone) being stronger than the northern component, contrary to observations, especially in the western part of this longitudinal range. This double ITCZ apparently resulted from the double latitudinal SST peak in this longitudinal range. East of 130°W to the coast of Central America in both FME1 and FME2, the single ITCZ north of the equator was near the latitude where the maximum SST resided. In the Atlantic in the JJA season, both FME1 and FME2 had an ITCZ at the correct latitude, but it was concentrated in the western Atlantic rather than in the eastern Atlantic as in the observations. In the DJF season, the ITCZ also resided close to the SST latitudinal peak in both FME1 and FME2

Thus we can conclude that in FME1 (EV=0) in both the JJA and DJF seasons, the control of the ITCZ latitudinal location by the SST peak is much stronger than the control by the earth's rotation. In other words, in Fig. 2b, curve R is relatively small compared with line S. This strong control by the SST peak is not changed much in FME2 (EV=1)

by adding rain re-evaporation. In summary, the problem described in subsection 3c of the ITCZ being too close to the equator occurred in FME1 in the regions where the SST peak was within 12° of the equator, and this problem was not alleviated by the rain re-evaporation introduced in FME2.

In separate experiments with the same model but with the horizontal resolution doubled, the wrong-hemisphere problem occurred over a very wide longitudinal domain--including the Indian Ocean--without rain re-evaporation, but was alleviated *with* rain re-evaporation (Figs. 6a and 6b), especially in the western Indian Ocean and over the maritime continent. The occurrence of the wrong-hemisphere problem (the double-ITCZ bias) as a result of increasing the horizontal resolution is consistent with our discussion in section 4 on the effect of increasing the horizontal resolution. The fact that adding rain re-evaporation helped alleviate the wrong-hemisphere problem in experiments with greater horizontal resolution indicates that the effect of rain re-evaporation is very much horizontal-resolution-dependent. The mechanism behind this dependence remains to be investigated. The too-close-to-the-equator problem did not appear in the Indian Ocean in either Fig. 6a or Fig. 6b. This is also consistent with our discussion in section 4 on the effects of increasing horizontal resolution.

In summary, FME1, FME2 and the experiments with higher horizontal resolution have verified that 1) the two types of ITCZ systematic errors--the wrong-hemisphere and the too-close-to-the-equator types--described in subsections 3b and 3c, respectively, indeed occur when the SST peak is close to the equator (within ~17° for the wrong-hemisphere type and within ~12° for the too-close-to-the-equator type) and 2) the ITCZ resides close to the SST peak when the latter is sufficiently away from the equator (>

~17° for the wrong-hemisphere type and > ~12° for the too-close-to-the-equator type). The fact that the wrong-hemisphere problem occurred in the experiments with higher horizontal resolution is consistent with our discussion in section 4. Our experiments also showed that the rain re-evaporation effect on the latitudinal location of the ITCZ is highly variable according to the model horizontal resolution.

FME3 (Fig. 7) showed that strengthening the northern SST peak and moving it farther north in the JJA season can move the ITCZ to the northern hemisphere in JJA. This is consistent with our discussion in section 3 in that if line S is given a greater slope and is moved northward far enough, there can be only a single ITCZ.

In FME4 (Fig. 8), the ITCZ precipitation showed no sign of a double ITCZ except for a small region around 170ºW, as a result of increasing RHc, which in turn resulted in curve R moving toward the long-dashed curve in Fig. 2c. There was only one intersecting point between curve R and line S either near the equator when the SST peak was near there--as in the western Pacific from 135°E to 170°W and in the Indian Ocean--or at about 10ºN--when the SST peak was near there--as in the eastern Pacific and in the Atlantic. This is consistent with our discussion in section 4.

5c. Discussion

The main objective of the above experiments is to provide support for the concepts presented in section 3. That goal, to a large extent, has been accomplished. These experiments also represent an initial push towards understanding the sensitivities of the ITCZ location and intensity to some modifications in the cumulus parameterization

scheme; but in this regard, our accomplishments are very limited. Nevertheless, it is important to point out that the concepts in sections 2 and 3 provide guidance in the effort to understand these sensitivities. To understand this guidance, it is best to use the aqua-planet settings first. Basically, since our theory points out that the latitudinal location of the ITCZ is the latitude where curve R and line S intersect (assuming the SST is zonally-uniform), the sensitivities of the ITCZ latitudinal location to changes in the GCMs can be studied by looking into the sensitivities of curve R and line S to these changes. Sensitivities of line S to changes in the GCMs can be determined by doing aqua-planet GCM experiments with the earth's rotation rate set at zero. From the sensitivities of the ITCZ and of line S to changes in the aqua-planet GCM the sensitivities of curve R can be determined, at least qualitatively. The sensitivities of curve R lead to the sensitivity of curve B (recall that R=A-B and that A is not sensitive to model changes.) Once the sensitivities of line S and curve B are obtained, their interpretations will be the objective of the study. Forming hypotheses to interpret the direction of sensitivities of line S and curve B may be a challenge, but it is not as difficult as explaining the sensitivity of curve B to a particular change relative to that of line S. The reason this relativity is important is that, as pointed out in Fig. 2c, it is curve B's strength *relative* to line S's strength that matters. Another factor that makes such an investigation more challenging is that these sensitivities are also functions of horizontal grid size. This is, of course, a result of the fact that the current cumulus parameterization schemes have not taken grid size into consideration. Investigating the sensitivities of the ITCZ location in a full GCM will be easier once the sensitivities in an aqua-planet version of the same GCM have been understood. In addition to the sensitivities of the ITCZ latitudinal location, there are the

sensitivities of the ITCZ intensity that need to be studied. In this regard, the guidance offered by the concepts in sections 2 and 3 is that the ITCZ intensity is related to the slope of the net forcing (R-S) at the latitude of the ITCZ. Through the sensitivity studies one can understand the impact of proposed model changes and strive to correct ITCZ systematic errors. Obviously, the work is quite sizeable and the experiments reported in this paper represent only an initial push.

We have done some additional experiments with regard to the sensitivity of line S to changes in rain re-evaporation and cumulus friction. In these experiments, using a Gaussian SST profile fixed in time without the earth's rotation, with and without rain re-evaporation, we found that the peak intensity of the zonally-averaged ITCZ precipitation--which is related to the slope of line S--weakens when rain re-evaporation is used. This outcome can be attributed to the fact that rain re-evaporation gives back to the atmosphere some of the rain water that would have reached the surface--and thereby reduces the intensity of convective heating and weakens the convective circulation. Adding cumulus momentum transport (or cumulus friction) has a similar impact due to the fact that cumulus friction impedes the convective circulation. This impact is, however, milder than that of rain re-evaporation. This last conclusion is based only on the formulations for rain re-evaporation and cumulus momentum flux used in the GMAO GCM.

6. Summary and remarks

The latitudinal location of the ITCZ over the ocean is controlled by the balance of two factors: the latitudinal distribution of the SST and the earth's rotation. The strength of each factor is affected by the model physics. Thus, the latitudinal location of the ITCZ responds to changes in the model physics. Identification of the origin of some of the ITCZ systematic errors in GCM simulations over the ocean--including the double ITCZ bias--and a description of how the treatment of the moist convective process can affect these errors have been the contribution of this paper and the work leading up to it.

The core contribution of this paper is section 3, which presents the concept embedded in Fig. 2c. This figure shows that relative to the control on the latitudinal location of the ITCZ by the SST peak--represented by line S (positive means northward attraction)--the control by the earth's rotation--represented by curve R (positive value means southward attraction)--can vary greatly and take on different shapes, depicted by different curves according to different model physics. The more serious systematic errors in the ITCZ latitudinal location in the JJA season fall into two types: 1) When curve R is close to the dotted-curve in Fig. 2c, a double ITCZ occurs where the component on the opposite side of the equator from the SST peak is stronger than the component on the same side of the equator as the SST peak. 2) When curve R falls between the two dashed curves in Fig. 2c, the ITCZ is too close to the equator. Neither type of error exists if the SST peak is located far enough away from the equator ($> \sim 17°$ for the first type and $> \sim 12°$ for the second type); but a relatively minor error can still occur. To achieve a good simulation of the ITCZ latitudinal location, curve R should be close to the solid curve in Fig. 2c. The experiments presented in section 5 have supported this core concept.

The intensity of the ITCZ in a setting with zonally-uniform SST is related to the latitudinal gradient of the net forcing on the ITCZ, R-S, at the latitude of the ITCZ. In a setting with zonally-non-uniform SST the presence of Walker circulation comes into play also. If the SST-peak controlling factor is greater than the rotational controlling factor in a GCM, the ITCZ precipitation in a zonally non-uniform setting tends to show excessive peaks in the zonal direction, generating locally-excessive precipitation maxima. Many GCMs show a strong dip in the ITCZ precipitation in the zonal direction in the middle of the eastern Pacific (e.g., Fig. 22 of Hack et al. 1998) because the control by the SST peak in the Pacific coastal region next to Central America is too high. Strong SST-peak control can also show up in the equatorial Indian Ocean and in the western Atlantic (Figs. 4a, 4b). As shown in Fig. 7, the greater the control by the SST peak relative to the rotational control, the worse the problem of excessive ITCZ precipitation concentration over local SST maxima in the equatorial regions. An obvious way to alleviate this problem is to reduce the SST-peak control by making the condition for the occurrence of parameterized cumulus convection less restrictive. Exactly how to accomplish this requires further study.

The impact of changes in rain re-evaporation and cumulus momentum transport on ITCZ systematic errors is highly variable. The ITCZ simulation may, in addition, be sensitive to other components of the model physics besides the cumulus parameterization (Chao and Chen 2004); however, they have not yet been systematically studied. The sensitivity of ITCZ systematic errors to horizontal resolution exists because the model physics is highly horizontal-resolution-dependent. Furthermore, the response to a change, or set of changes, in the model physics can be very different--even in opposite

directions--in different geographical areas, due to different regional and temporal SST distributions.

How to change the GCM physics so as to improve the ITCZ precipitation simulation remains a challenge, despite the conceptual advances made herein. Although we have identified a few factors in the model physics that may influence the ITCZ precipitation simulation, we have not yet identified all the factors. Also, we have not yet completely explained the mechanisms behind the effects of these factors. Moreover, our discussion of the effects of these factors, as presented in section 4, centers on their impact on the intensity of synoptic-scale convective systems; there may be other aspects of synoptic systems, such as size and life cycle, that are changed by changing these factors.

Among the few important factors that we are familiar with, we do not yet know to what degree each of them should be changed. There may be sets of changes to these factors that can bring a similar degree of improvement in the ITCZ precipitation simulation. The best choice among these sets of changes will have to be determined by--in addition to the model's performance in simulating the monthly and seasonal mean structure of the ITCZ precipitation--the model's performance in simulating phenomena related to the ITCZ, such as the Madden-Julian oscillation, mixed Rossby-gravity (Yanai) waves, Kelvin waves, and the ITCZ breakdown-and-zonalization cycle (all related to the oscillations of convection within the ITCZ). Thus, the physical mechanisms behind these other tropical phenomena should also be studied in order to improve the GCM simulation of ITCZ precipitation. In other words, possible sources of the systematic errors in the GCM tropical circulation simulation in the wavenumber-frequency domain and the mechanisms behind these errors should be studied in conjunction with the study of GCM

ITCZ precipitation systematic errors, since current GCMs exhibit considerable difficulty simulating the wave number-frequency power spectrum of tropical large-scale waves (Lin, et al. 2006). Therefore, much more work lies ahead.

Although recent efforts in super-parameterization have resulted in improvement in the ITCZ precipitation simulation, there is room for further improvement. For example, the too-high precipitation maximum in the northwestern Pacific in JJA is still present in the latest models with super-parameterization (Tao, personal communication).

This study is based on aqua-planet settings with prescribed SST; the roles of land-atmosphere and ocean-atmosphere interactions in determining ITCZ precipitation will be among our future research topics, since many ITCZ precipitation problems related to landmass and air-sea interaction still exist. For example, the coastal regions of South America and India are often among the trouble spots for GCM precipitation simulation. The missing ITCZ in the African coastal region from Guinea to Nigeria--which may be related to the precipitation over-concentration in the western Atlantic as shown in Figs. 4a and 4b--is another example of an ITCZ precipitation simulation problem. Improving the El Nino simulation, which strongly depends on the ITCZ precipitation simulation, remains a challenge as well.

Acknowledgments

This work was supported by the Modeling, Analysis and Prediction program of NASA Science Mission Directorate.

APPENDIX A

Comments on Curve B in Fig. 1

Fig. 11 of Chao and Chen (2004) explains the origin of curve B in Fig. 1. Curve B is defined mathematically as the latitudinal gradient of $\alpha^2 N,^2$ where α is the ratio of the vertical scale to the horizontal scale of the convective circulation and N^2 is the vertical stability. As explained in Chao and Chen (2004, page 451), N^2 is the vertical stability according to the model's cumulus parameterization scheme, and it is a function of the vertical profiles of temperature and mixing ratio. Both profiles are affected by surface heating fluxes, which are in turn affected by Coriolis parameter-modified surface winds. Also, surface winds in a convective system are highly related to the cumulus parameterization scheme in a GCM. Since the cumulus parameterization scheme--not to mention other model physics components--has no simple analytic formula, curve B has no simple analytic formula. Therefore, curve B can only be obtained through GCM experiments. Once curve B is obtained experimentally, one should then try to explain it in order to have a complete theory of ITCZ latitudinal location.

The experimental method to obtain curve B is first to determine A-B, which is curve R in Figs. 2a and 2b of this paper (or curve A in Fig. 8 of Chao 2000). The way to determine curve R has been explained in Chao (2000)—i.e., by moving the SST profile meridionally while retaining its shape and tracing the location of the ITCZ. Of course, with curve A in Fig. 1 known analytically, and with A-B (=R) obtained experimentally, curve B can be obtained experimentally. Due to the consideration stated in Appendix B, curve R cannot be determined exactly, but it can be obtained to a good approximation. Therefore, Figs. 1 and 2 are schematic diagrams rather than precise experimental results.

As stated in Chao and Chen (2004, see its Fig. 11), curve B represents the poleward attraction on the convective systems (which are the elements of the ITCZ) due to Coriolis parameter-modified surface fluxes, which affect N.[2] Thus, we can consider the poles the center of the attractor, with the magnitude of the attraction being larger as one moves away from the poles. This is depicted by the dashed curve in Fig. 16 of Chao and Chen (2004). The text associated with that figure also explains why curve B has a peak at around 10°N. Why curve B has a rapid drop around 18°N has not been explained, and this is a topic that we are still studying. Our current thinking is that the answer has to do with the variation in size of the convective systems within the ITCZ as a function of the Coriolis parameter (or as a function of latitude). In the meantime, we have to be content with the knowledge that curve B can be obtained experimentally and it, therefore, must be correct.

The fact that we have not completely explained curve B does not imply that Fig. 1 is of no use. Fig. 1 was used to explain why the speed of transition from a single ITCZ over the equator to a double ITCZ (though one of its two components did not show up) is different from the speed of transition in the reverse direction in Figs. 2 and 3 of Chao and Chen (2004).

APPENDIX B

The Additive Assumption in Fig. 2

In Fig. 2, it is assumed that the two types of attractions on the ITCZ due to the earth's rotation and the SST peak, respectively, can be added. This additive assumption is only approximately correct; however, our explanation of the latitudinal location of the ITCZ does not depend on this assumption being exactly correct. This appendix provides a discussion of this point.

The ITCZ latitudinal location can be expressed as the latitude(s) where $A(\Omega,\mathrm{SST},\phi)=0$ and $\partial A/\partial\phi>0$, where A denotes the net southward attraction on the ITCZ. A is, of course, a highly nonlinear function of the earth's rotation rate Ω, SST distribution, and latitude ϕ, among other factors. This equation can only be approximately expressed as $A(\Omega, \mathrm{G}, \phi) + A(0, \mathrm{SST}, \phi)=0$, where G is the globally-averaged SST—or curve R minus line S=0 in Fig. 2.

Our argument in explaining Fig. 3 of Chao and Chen (2001) using Fig. 2b of this paper only requires the fact that as the SST peak is moved northward from the equator, the two ITCZ components move northward as well. The locations of these ITCZ components do not have to be at the exact locations of the intersecting points between curve R and line S in Fig 2. Our argument as to why the southern ITCZ component should be stronger than the northern ITCZ component once the SST peak moves into the northern hemisphere does not depend on the additive assumption being exactly correct

because if it were exactly correct, the southern ITCZ component would not reach the equator in Fig. 3 of Chao and Chen (2001).

These considerations also reveal that Fig. 2 of Chao and Chen (2001) is not correct. That figure was constructed in an attempt to follow the additive assumption exactly, but it failed to do so completely, and had to incorporate an erroneous discontinuity. It should be replaced by Fig. 2.b of this paper. Also note that Fig. 6 of CC01 has been superseded by Fig. 15 of CC04, which is reproduced as Fig. 1.

APPENDIX C

The Sudden Movement toward the Equator in Fig. 1 as RHc Is Increased

According to our Fig. 1, when the critical boundary layer relative humidity, RHc, is increased (equivalently, when Bras is moved toward Bmca) the double ITCZ, in the case when the SST and solar angle are both globally uniform, first moves toward the equator slowly and then is expected to transition abruptly to a single ITCZ over the equator. However, Fig. 2 of Chao and Chen (2004) does not show such *abrupt* movement. At this time, we can only provide some speculative discussion about this. In Fig. 2 of Chao and Chen (2004) in the equatorial regime after the transition (i.e., after day 300) or in Fig. 3 of Chao and Chen (2004) before day 200 the rainfall pattern is not exactly a single peak at the equator; the peak at the equator is sometimes split into two peaks and there are often secondary peaks at about 22N&S (although time and zonally averaged precipitation in this regime shows a single peak (see the short dash line of Fig. 7 of Chao and Chen (2001)). Thus, our speculative answer is that the complex precipitation pattern in the equatorial regime, whose cause is a puzzle, might have prevented the anticipated abrupt movement to the equator (see the note below). All these do not mean that Fig. 1 is incorrect. The experiments in Chao (2000) showed that curve R, representing the net southward attraction due to the earth's rotation, for MCA is zero at the equator, it rises with the latitude and then falls to a minimum around 13N and then rises sharply. This behavior of curve R is consistent with the difference between curve A and curve Bmca in Fig. 1. Thus, Fig. 1 is not wrong, it just needs refinement, which hopefully we can do in the future.

Note: When the SST is giving a Gaussian latitudinal profile with its peak at the equator, the precipitation pattern of the equatorial regime is a simple lone peak over the equator, instead of that kind of complex pattern, as indicated in the beginning days of Fig 11 of Chao and Chen (2001) and as indicated at the end of the first 4 months of Fig. 3a of this paper. In Fig. 2c the angle between line S and the long dashed curve, which overlies

the horizontal axis, becomes much smaller, when the slope of line S is reduced to zero (i.e., when SST is globally uniform). When this angle becomes smaller, the stability of the ITCZ at the equator becomes weaker and secondary instability can thus have a chance to emerge. This gives the hint that the complex equatorial pattern is a secondary instability, which can be suppressed, when the primary stability is strong.

References

Bacmeister, J. T., M. J. Suarez, and F. R. Robertson, 2006: Rain re-evaporation, boundary-layer/convection interactions, and Pacific rainfall patterns in an AGCM. *J. Atmos. Sci.*. **63**, 3383-3403.

Barsugli, J., S.-I Shin, and P. D. Sardeshmukh, 2005: Tropical climate regimes and global climate sensitivity in a simple setting. *J. Atmos. Sci.*, **62**, 1226-1240.

Chao, W. C., 2000: Multiple quasi-equilibria of the ITCZ and the origin of monsoon onset. *J. Atmos. Sci.*, **57**, 641-651.

Chao, W. C., and B. Chen, 2001: Multiple quasi-equilibria of the ITCZ and the origin of monsoon onset. Part II. Rotational ITCZ attractors. *J. Atmos. Sci.,* **58**, 2820-2831.

Chao, W. C., and B. Chen, 2004: Single and double ITCZ in an aqua-planet model with constant SST and solar angle. *Climate Dynamics*, **22**, 447-459.

Chou, M. D., and M. J. Suarez, 1994: An efficient thermal infrared radiation parameterization for use in general circulation models. NASA Tech. Memo, 104606, **10**, 84pp.

Chou, M. D., and M. J. Suarez, 1999: A solar radiation parameterization for atmospheric studies, NASA Technical Memo, 104606, Vol. 11, 40pp.

de Szoeke, S. P., Y. Wang, S.-P. Xie, and T. Miyama, 2006: Effect of shallow cumulus convection on the eastern Pacific climate in a coupled model, *Geophys. Res. Lett.*, **33**, L17713, doi:10.1029/2006GL026715.

de Szoeke, S. P. and S.-P. Xie, 2008: The tropical eastern Pacific seasonal cycle Assessment of errors and mechanisms in IPCC AR4 coupled ocean-atmosphere general circulation models. J. Climate, submitted.

Hack, J. J., J T. Kiehl and J. W. Hurrell, 1998: The hydrologic and thermodynamic characteristics of the NCAR CCM3. *J. Clim.*, **11**, 1179-1206.

Hess, P. G., D. S. Battisti and P. J. Rasch, 1993: Maintenance of the intertropical convergence zone and the tropical circulation on a water-covered earth. *J. Atmos. Sci.*, **50**, 691-713.

Jung, J. H., and A. Arakawa, 2004: The resolution dependence of model physics: Illustration from nonhydrostatic model experiments. *J. Atmos. Sci.*, **61**, 88-102.

Kirtman B. P., and E. K. Schneider, 2000: A spontaneously generated tropical atmospheric general circulation. *J. Atmos. Sci.*, **57**, 2080-2093.

Koster, R., and M. Suarez, 1996: Energy and water balance calculations in the Mosaic LSM. *NASA Tech Memo*. 104606, Vol. 9, 60 pp. (available from the library of NASA/Goddard Space Flight Center, Greenbelt, MD 20771).

Lin, J. et al., 2006: Tropical intraseasonal variability in 14 IPCC AR4 climate models. Part I: Convective signals. *J. Climate*, **19**, 2665-2690.

Lin, J., 2007: The double ITCZ problem in IPCCAR4 coupled GCMs: Ocean-atmosphere feedback analysis. *J. Climate*, 20, 4497–4525.

Lin, S.-J. 2004: A "vertically Lagrangian" finite-volume dynamical core for global models. *Mon. Wea. Rev.,* **132**, 2293–2307.

Lindzen, R. S., and S. Nigam, 1987: On the role of sea-surface temperature gradients in forcing low-level winds and convergence in the tropics. *J. Atmos. Sci.*, **44**, 2418-2436.

Lock, A. P., A. R. Brown, M. R. Bush, G. M. Martin, and R. N. B. Smith, 2000: A new boundary layer mixing scheme. Part I: Scheme description and single-column model tests. *Mon. Wea. R*ev., **128**, 1387-1399.

Louis, J.-F., 1979: A parametric model of vertical eddy fluxes in the atmosphere. *Boundary Layer Meteor*. **17**, 187-202.

Manabe, S., J. Smagorinsky, and R. F. Strickler, 1965: Simulated climatology of a general circulation model with a hydrological cycle. *Mon. Wea. Rev.*, **93**, 769-798.

Moorthi, S., and M. J. Suarez, 1990: Relaxed Arakawa-Schubert: A parameterization of moist convection for general circulation models. *Mon. Wea. Rev.,* **120**, 978-1002.

Philander, S. G. H., D. Gu, D. Halpern, G. Lambert, N.C. Lau, T. Li, R. C. Pacanowski, 1996: Why the ITCZ is mostly north of the equator. *J. Climate*, **9**, 2958-2972

Pike, A. C., 1971: Intertropical convergence zone studied with an interacting atmosphere and ocean model. *Mon. Wea. Rev*., **99**, 469-477.

Raymond, D. J., 2000: The Hadley circulation as a radiative-convective instability. *J. Atmos. Sci*., **57**, 1286-1297.

Sumi, A., 1992: Pattern formation of convective activity over the aqua-planet with globally uniform sea surface temperature. *J. Meteor. Soc. Japan*, **70**, 855-876.

Xie, P., and P. A. Arkin, 1998: Global monthly precipitation estimates from satellite-observed outgoing longwave radiation. *J. Climate,* **11**, 137–164.

Wu, X., X. Liang, and G. J. Zhang, 2003: Seasonal migration of ITCZ precipitation across the equator: Why can't GCMs simulate it? *GRL*, **30**, No. 15, 1824-1828.

Zhang, G. J., and H. Wang, 2006: Toward mitigating the double ITCZ problem in NCAR CCSM3. *Geophys. Res. Let.*, **33**, L060709, Doi:10.1029/2005GL025229.

Table 1. Aqua-planet experiment results from May 1 to December 31 as a function of EV and CF. Single (double) means the ITCZ remained single (double). Names of the months signify experiments that yielded a double ITCZ where the southern component crossed the equator during the specified month.

	EV					
\	0	0.5	0.75	1.0	1.5	2.0
CF						
0	single	single	June	August	double	
1		single	Aug	Sept	Sept	Sept

Figure Captions

Fig. 1 Schematic diagram showing the strength of the two types of attraction acting on the ITCZ due to the earth's rotation. Curve A represents the strength of the southward attraction due to inertial stability. Curve B represents the strength of the northward attraction due to the latitudinal gradient of f-modified surface fluxes associated with synoptic-scale convective systems. Point P denotes the intersection between curve A and curve B_{RAS}. (Fig. 15 of Chao and Chen 2004)

Fig. 2a Curve R represents the net southward attraction on the ITCZ due to the earth's rotation--i.e., the difference between the two curves in Fig. 1 when MCA is used--and line S represents the northward attraction on the ITCZ due to an SST peak at 17°N. Line S intersects curve R at three points. Line S1 is line S when the SST peak is close to the equator. (Fig. 8a of Chao 2000)

Fig. 2b Curve R represents the strength of the southward net attraction on the ITCZ due to the earth's rotation--i.e., the difference between the two curves in Fig. 1 when RAS is used--and line S represents the strength of the northward attraction on the ITCZ due to the SST peak when the SST peak is at the equator.

Fig. 2c Curve R, relative to line S, has different shapes corresponding to various magnitudes of curve B in Fig. 1. The solid curve R represents the situation in nature.

Fig. 3a Zonally-averaged precipitation (mm/day) for AE0.5C0 as a function of latitude and time.

Fig. 3b Zonally-averaged precipitation (mm/day) for AE0.75C1 as a function of latitude and time.

Fig. 4a June-July-August mean precipitation (mm/day) in 1993 for FME1.

Fig. 4b June-July-August mean precipitation (mm/day) in 1994 for FME1.

Fig. 4c December-January-February mean precipitation (mm/day) in 1993 for FME1.

Fig. 4d December-January-February mean precipitation (mm/day) in 1994 for FME1.

Fig. 4e June-July-August mean surface temperature (°K), which is SST over the oceans, in 1993 for FME1.

Fig. 4f June-July-August mean surface temperature (°K), which is SST over the oceans, in 1994 for FME1.

Fig. 4g June-July-August mean precipitation (mm/day) in 1993 from Xie-Arkin (1998) dataset.

Fig. 4h June-July-August mean precipitation (mm/day) in 1994 from Xie-Arkin (1998) dataset.

Fig. 5a June-July-August mean precipitation (mm/day) in 1993 for FME2.

Fig. 5b June-July-August mean precipitation (mm/day) in 1994 for FME2.

Fig. 5c December-January-February mean precipitation (mm/day) in 1993 for FME2.

Fig. 5d December-January-February mean precipitation (mm/day) in 1994 for FME2.

Fig. 6a June-July-August mean precipitation (mm/day) in 1995 without rain re-evaporation in an experiment with horizontal resolution doubled.

Fig. 6b Same as Fig. 6.a but with rain re-evaporation.

Fig. 7 June-July-August mean precipitation (mm/day) in 1993 for FME3.

Fig. 8 June-July-August mean precipitation (mm/day) in 1993 for FME4.

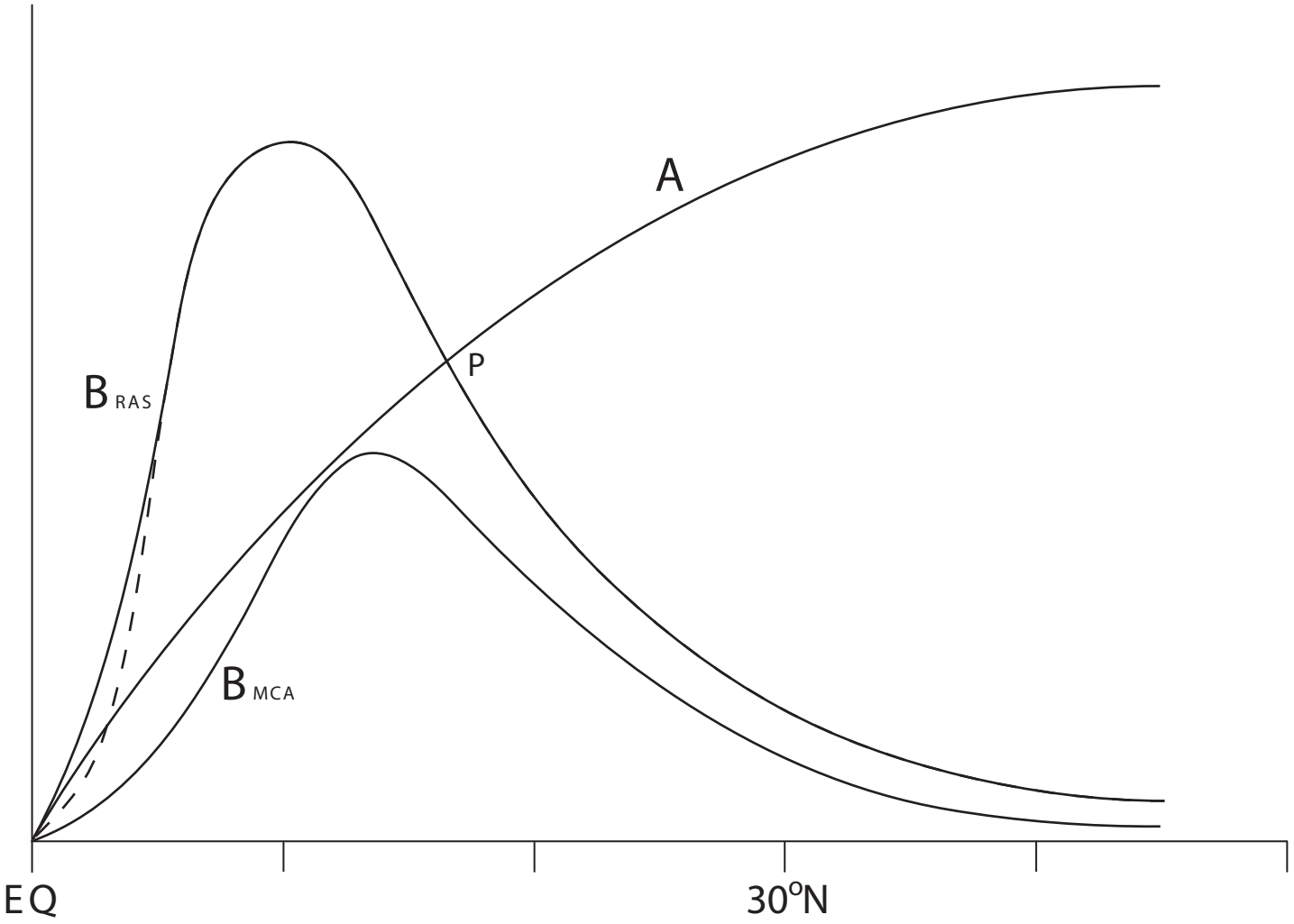

Fig. 1 Schematic diagram showing the strength of the two types of attraction acting on the ITCZ due to the earth's rotation. Curve A represents the strength of the southward attraction due to inertial stability. Curve B represents the strength of the northward attraction due to the latitudinal gradient of f-modified surface fluxes associated with synoptic-scale convective systems. Point P denotes the intersection between curve A and curve BRAS. (Fig. 15 of Chao and Chen 2004)

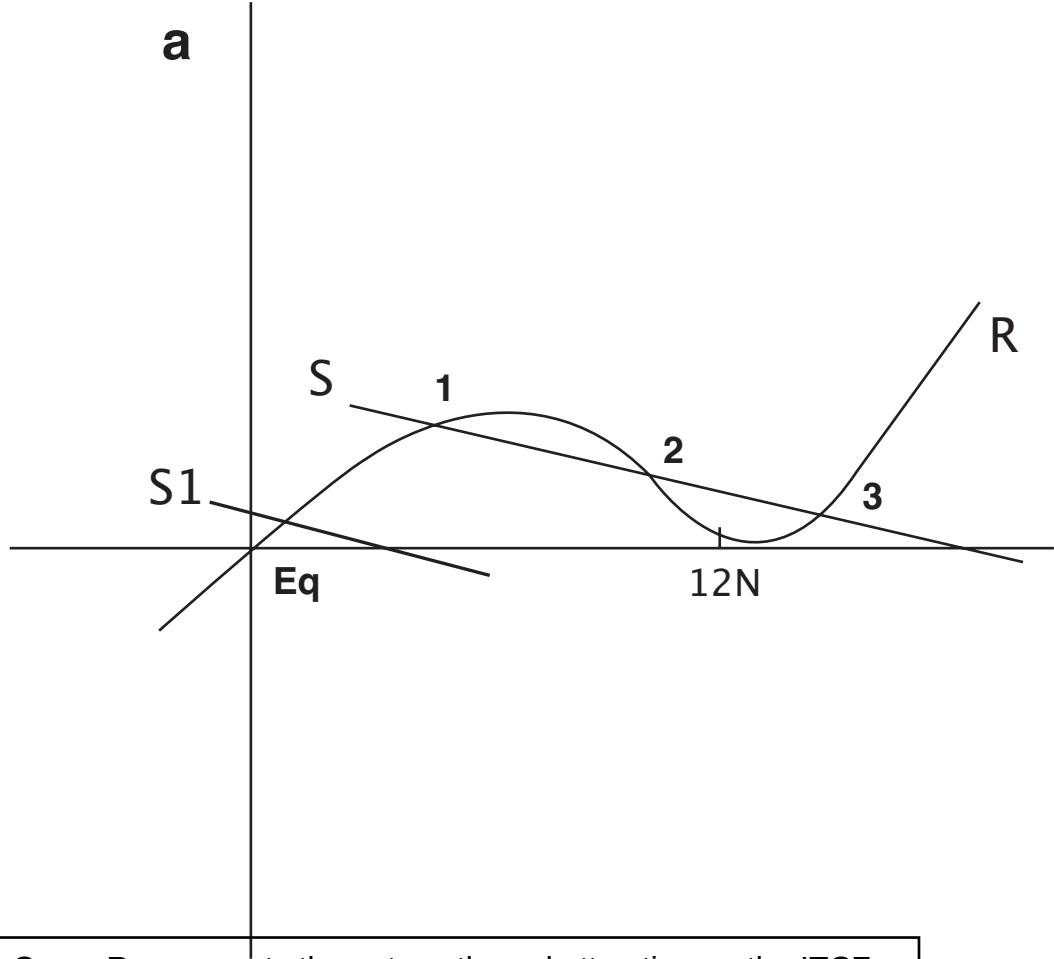

Fig. 2a Curve R represents the net southward attraction on the ITCZ due to the earth's rotation--i.e., the difference between the two curves in Fig. 1 when MCA is used--and line S represents the northward attraction on the ITCZ due to an SST peak at 17•N. Line S intersects curve R at three points. Line S1 is line S when the SST peak is close to the equator. (Fig. 8a of Chao 2000)

A1408.004

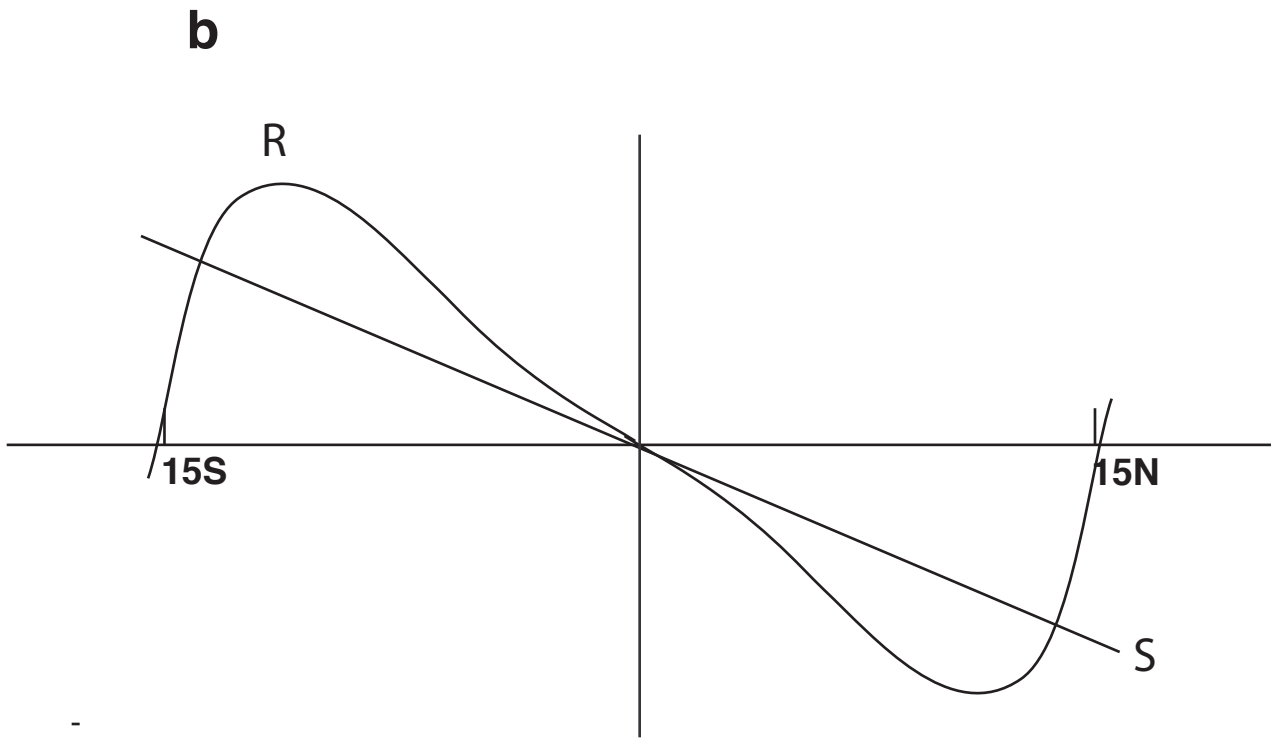

Fig. 2b Curve R represents the strength of the southward net attraction on the ITCZ due to the earth's rotation--i.e., the difference between the two curves in Fig. 1 when RAS is used--and line S represents the strength of the northward attraction on the ITCZ due to the SST peak when the SST peak is at the equator.

A1408.03a

C

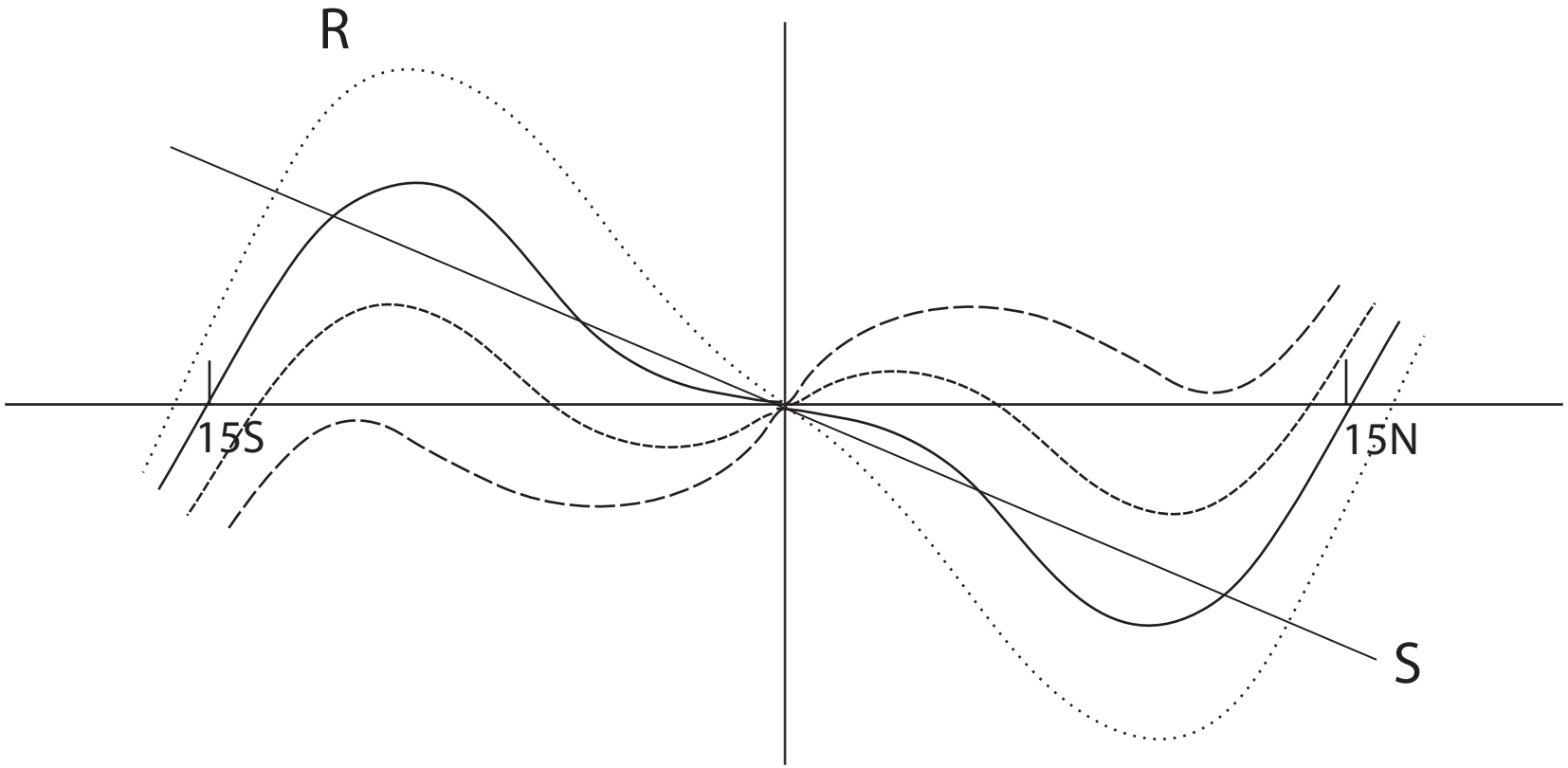

Fig. 2c Curve R, relative to line S, has different shapes corresponding to various magnitudes of curve B in Fig. 1. The solid curve R represents the situation in nature.

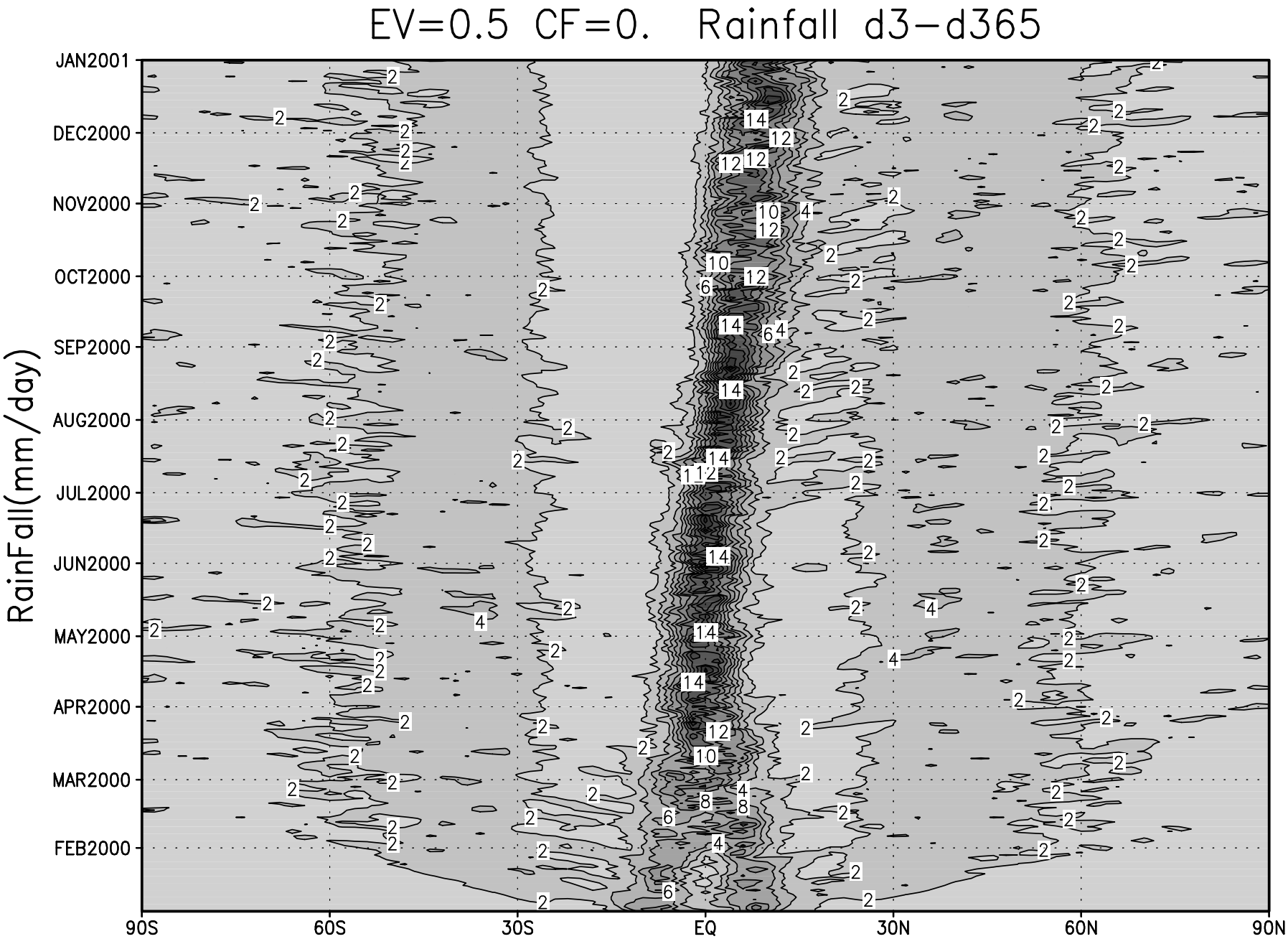

Fig. 3a Zonally-averaged precipitation (mm/day) for AE0.5C0 as a function of latitude and time.

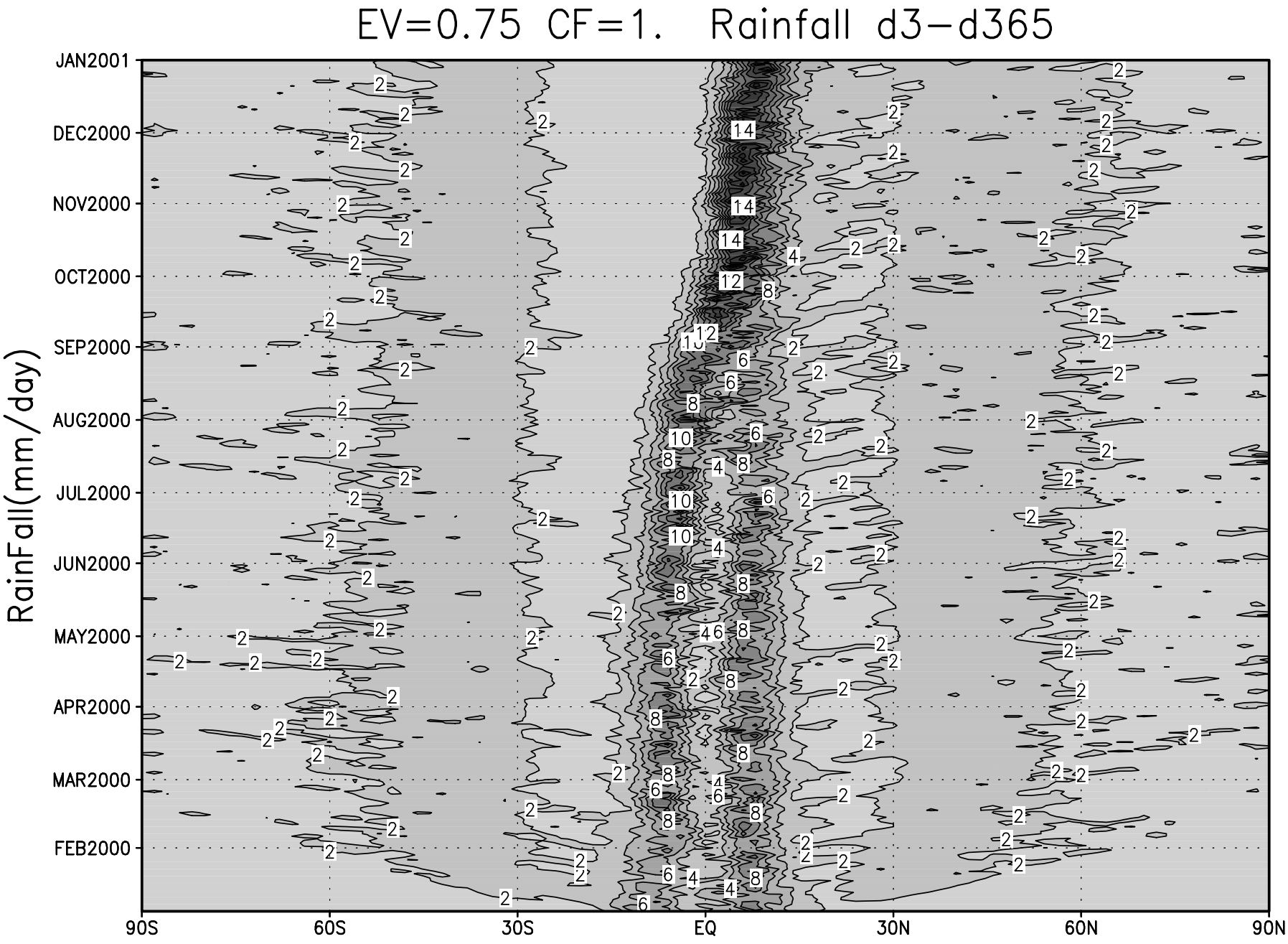

Fig. 3b. Zonally-averaged precipitation (mm/day) for AE0.75C1 as a function of latitude and time.

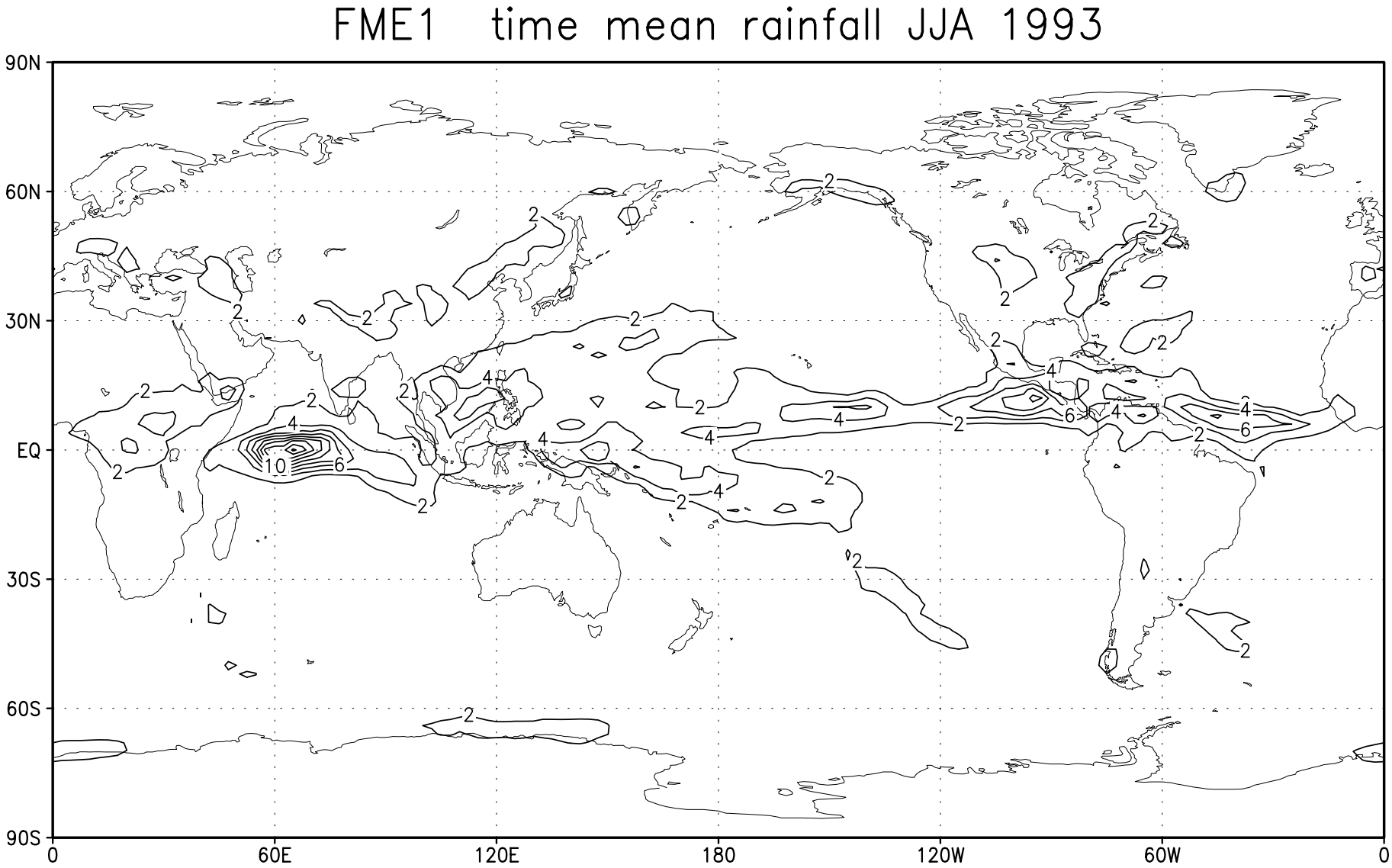

Fig. 4a June-July-August mean precipitation (mm/day) in 1993 for FME1.

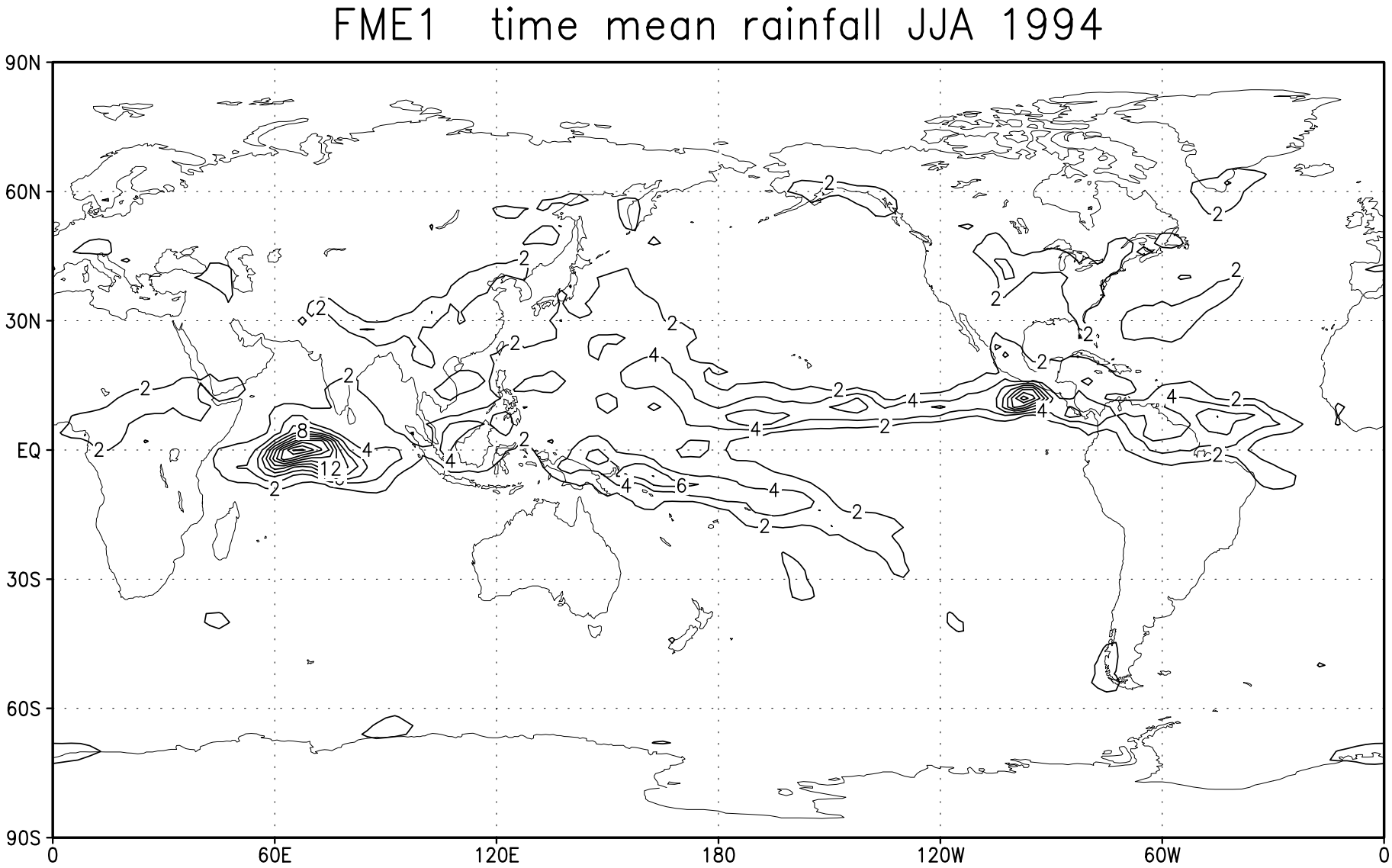

Fig. 4b June-July-August mean precipitation (mm/day) in 1994 for FME1.

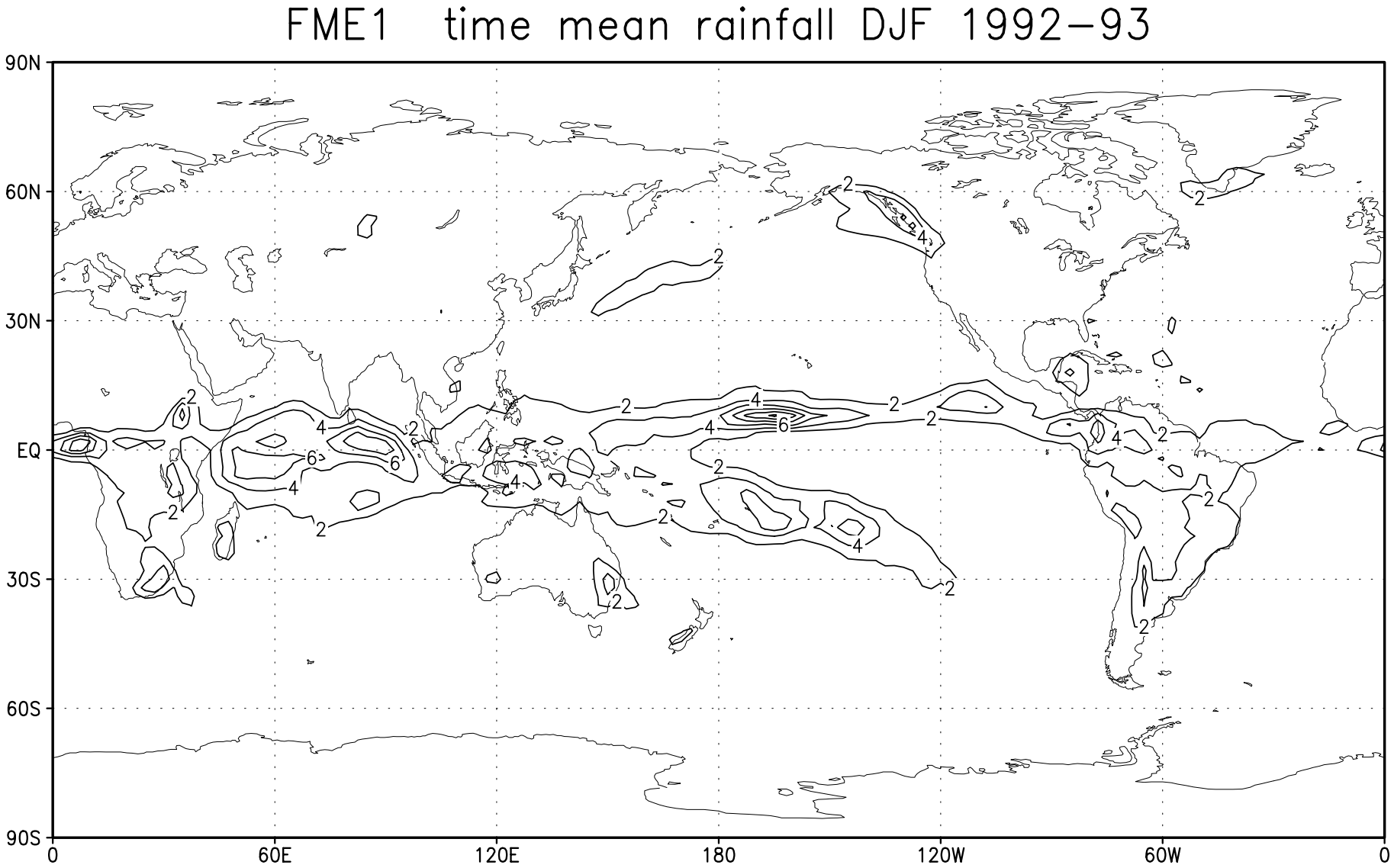

Fig. 4c December-January-February man precipitation (mm/day) in 1992-93 for FME1.

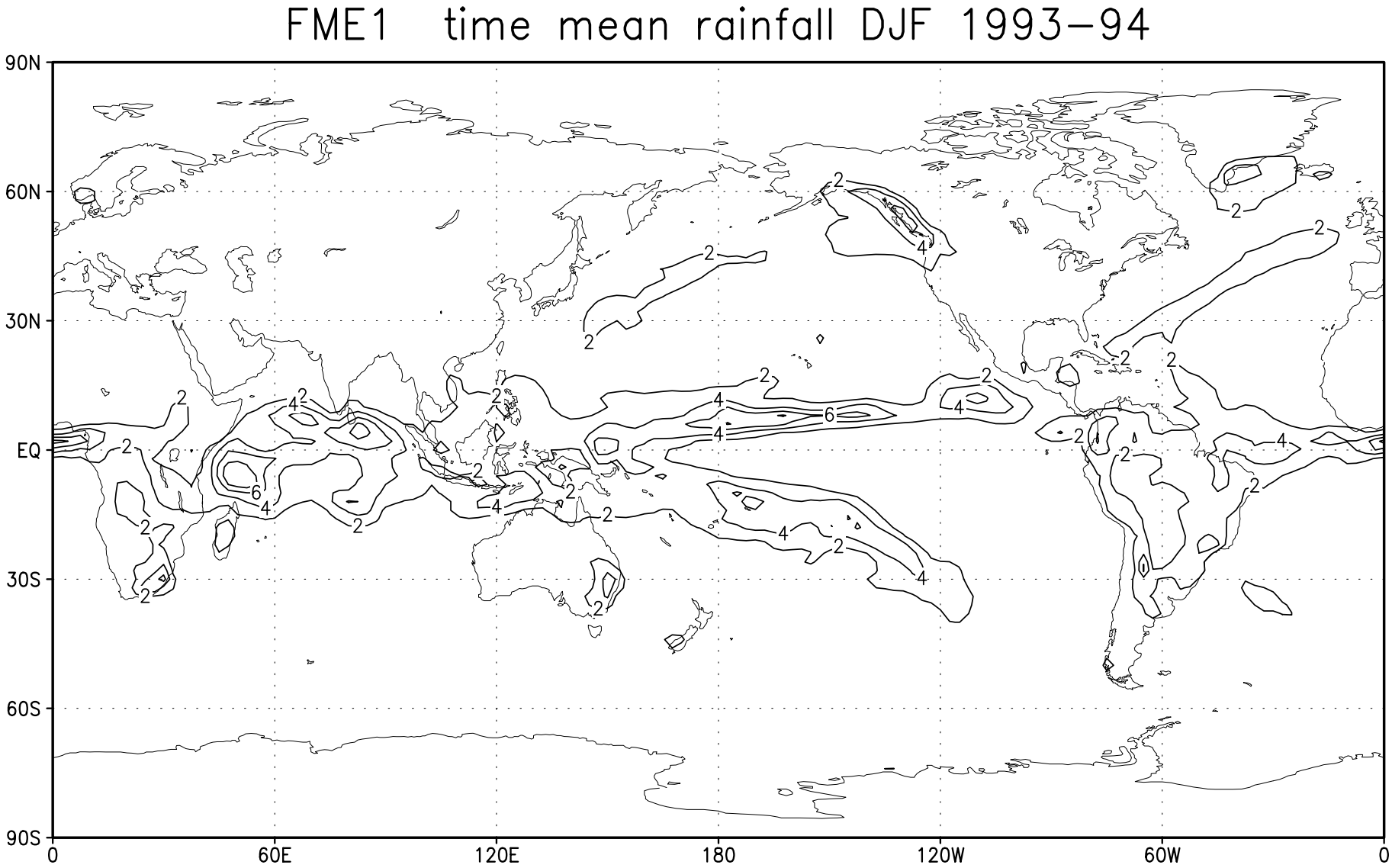

Fig. 4d December-January-February mean precipitation (mm/day) in 1993-94 for FME1.

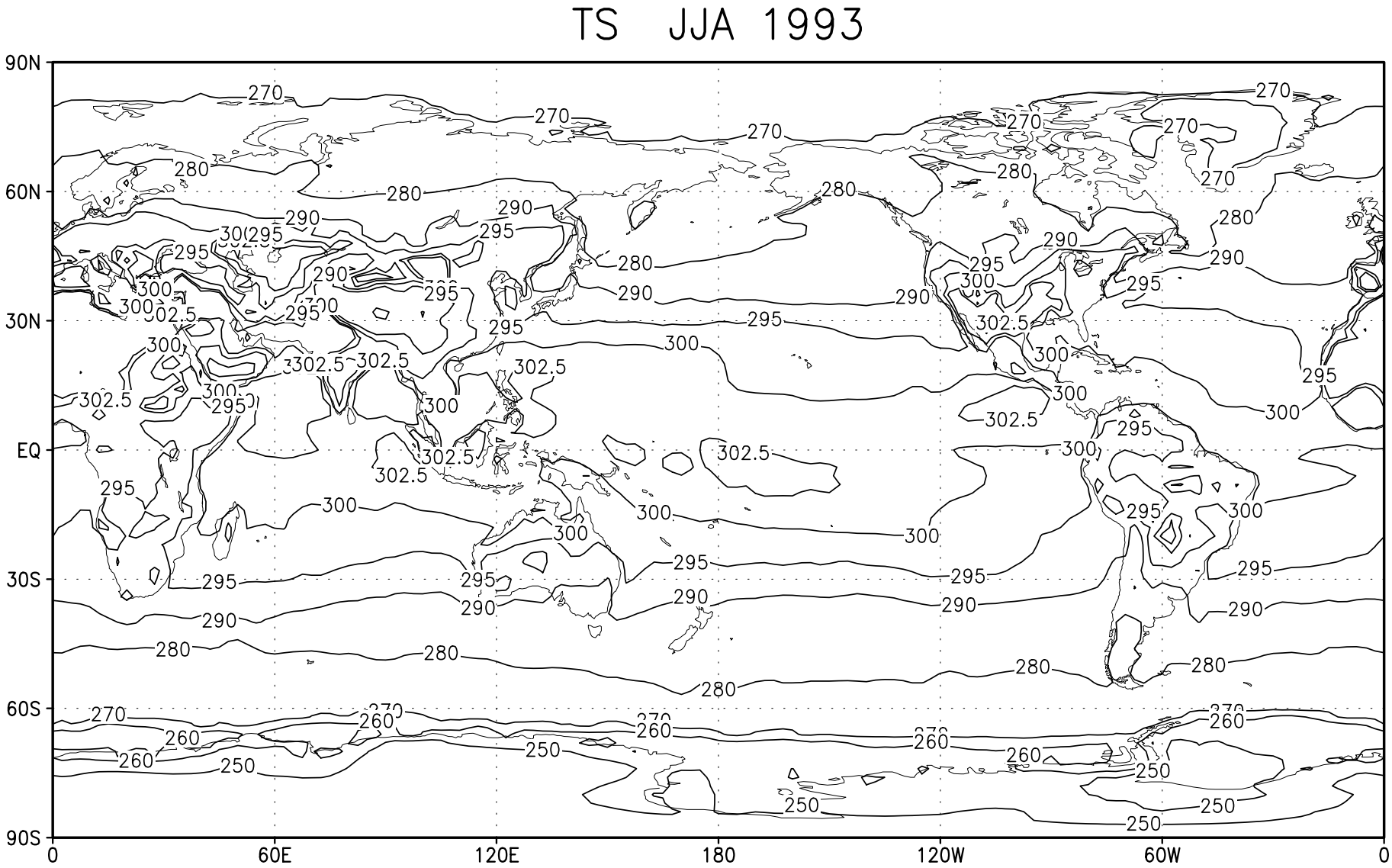

Fig. 4e June-July-August mean surface temperature (K), which is SST over the oceans, in 1993 for FME1.

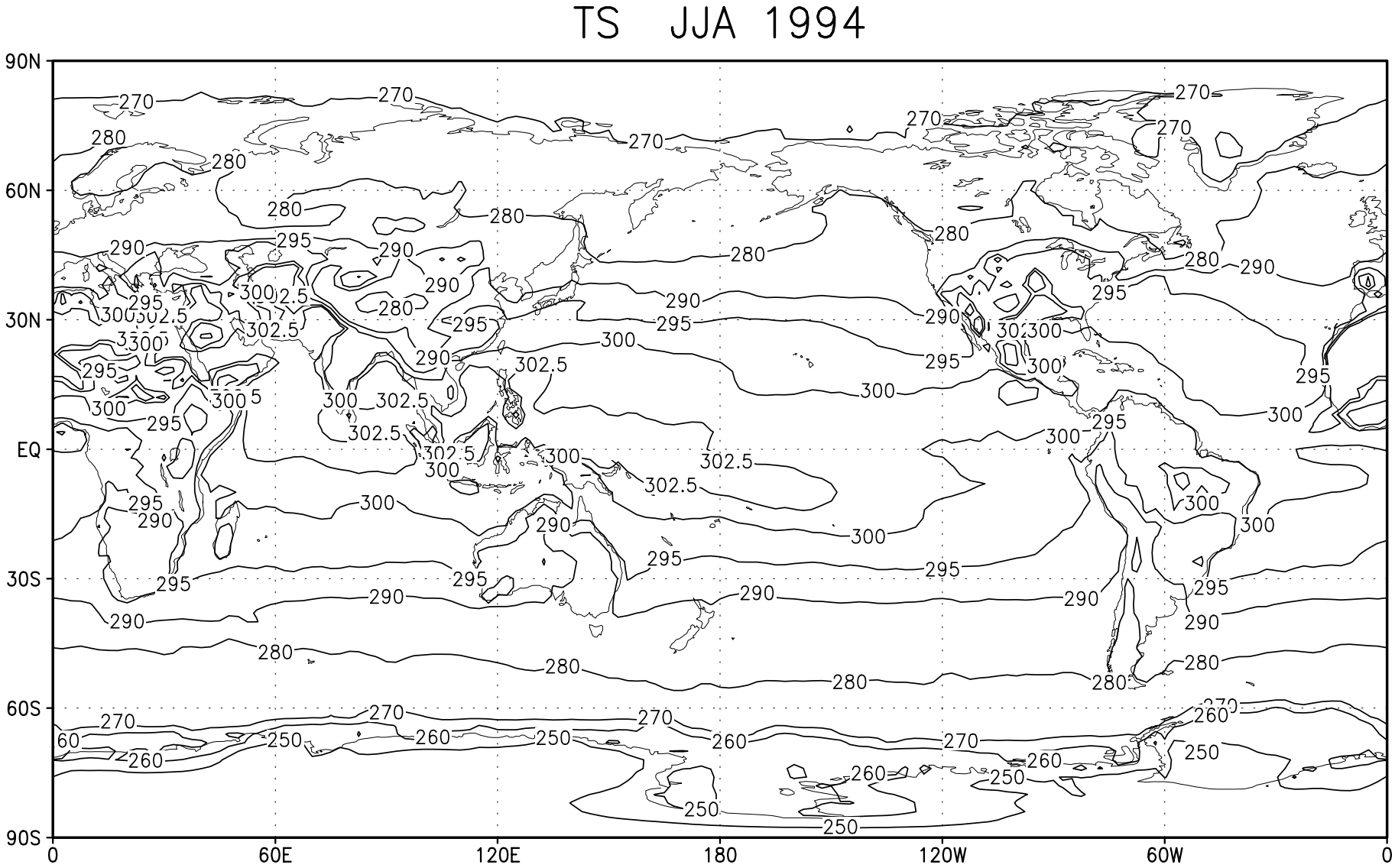

Fig. 4f June-July-August mean surface temperature (K), which is SST over the oceans, in 1994 for FME1.

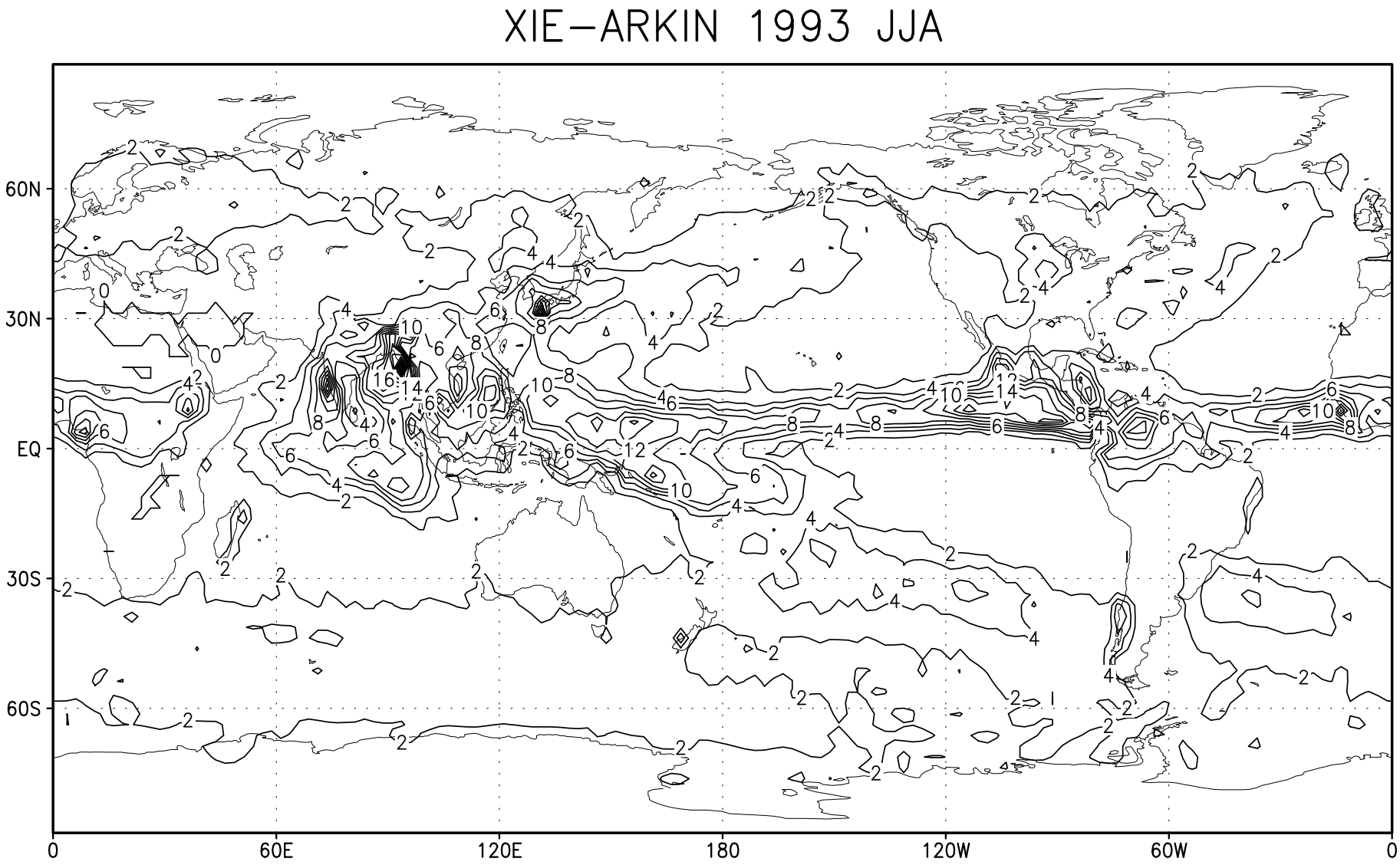

Fig. 4g June-July-August mean precipitation (mm/day) in 1993 from Xie-Arkin data.

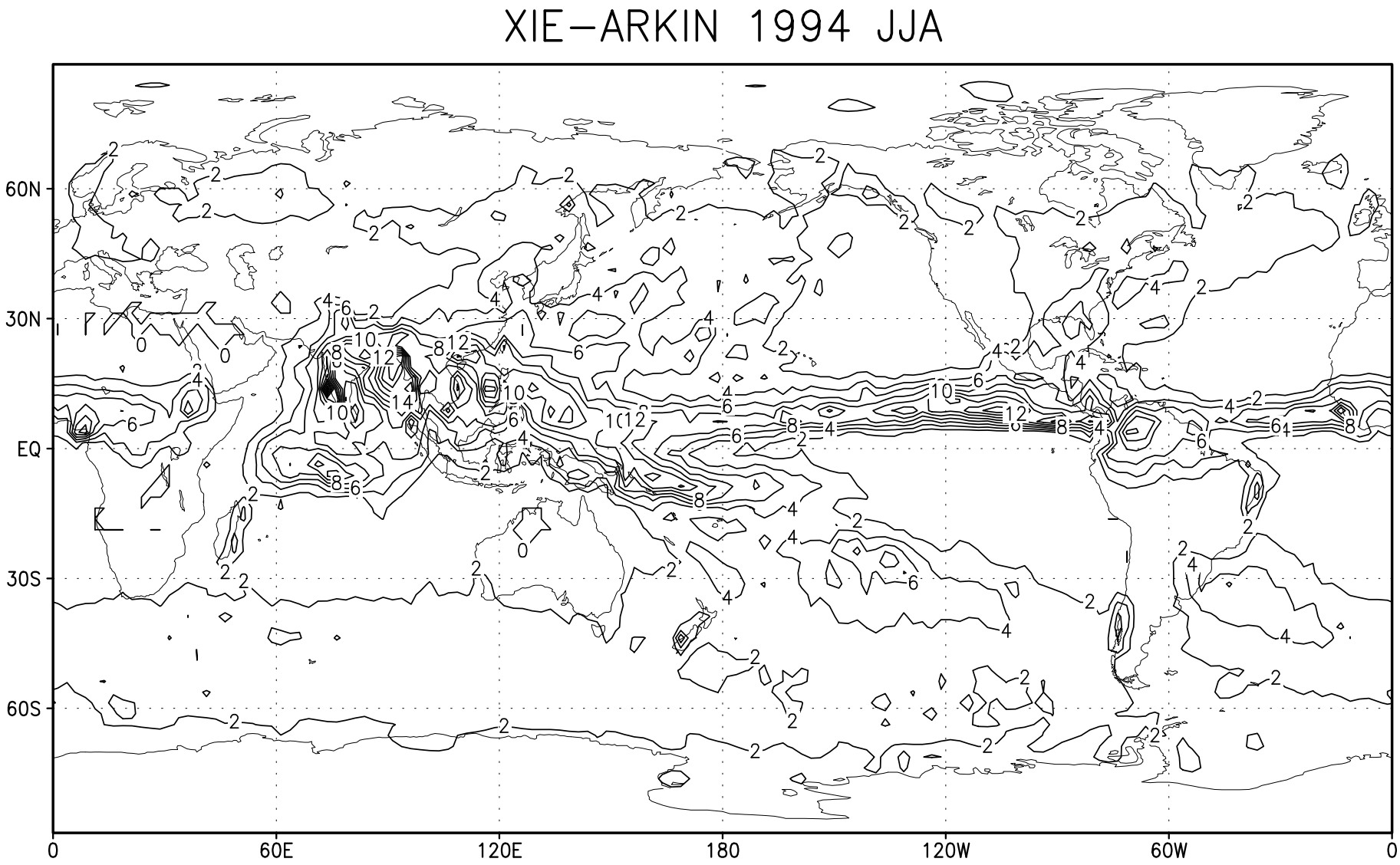

Fig. 4h June-July-August mean precipitation (mm/day) in 1994 from Xie-Arkin data.

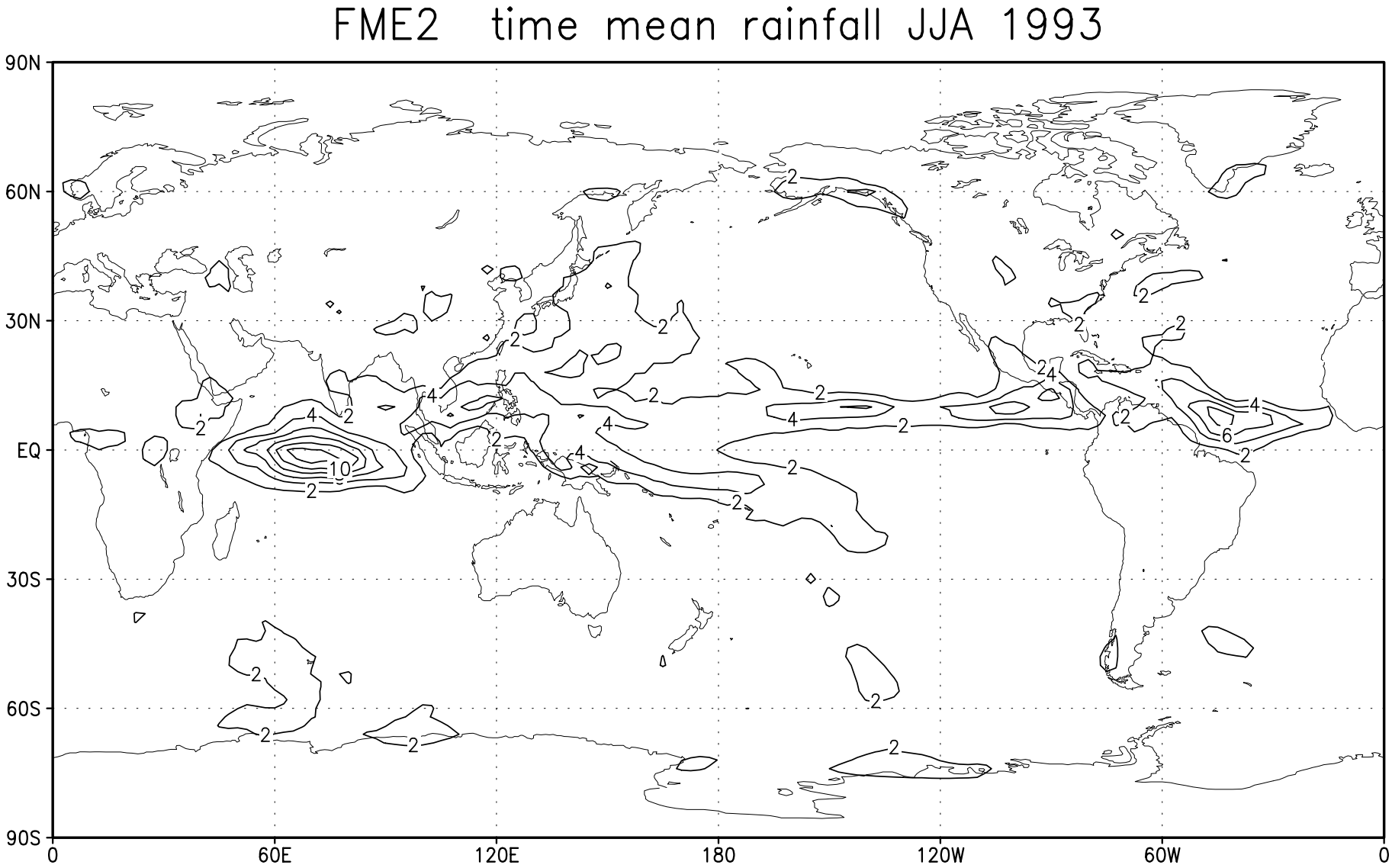

Fig. 5a June-July-August mean precipitation (mm/day) in 1993 for FME2.

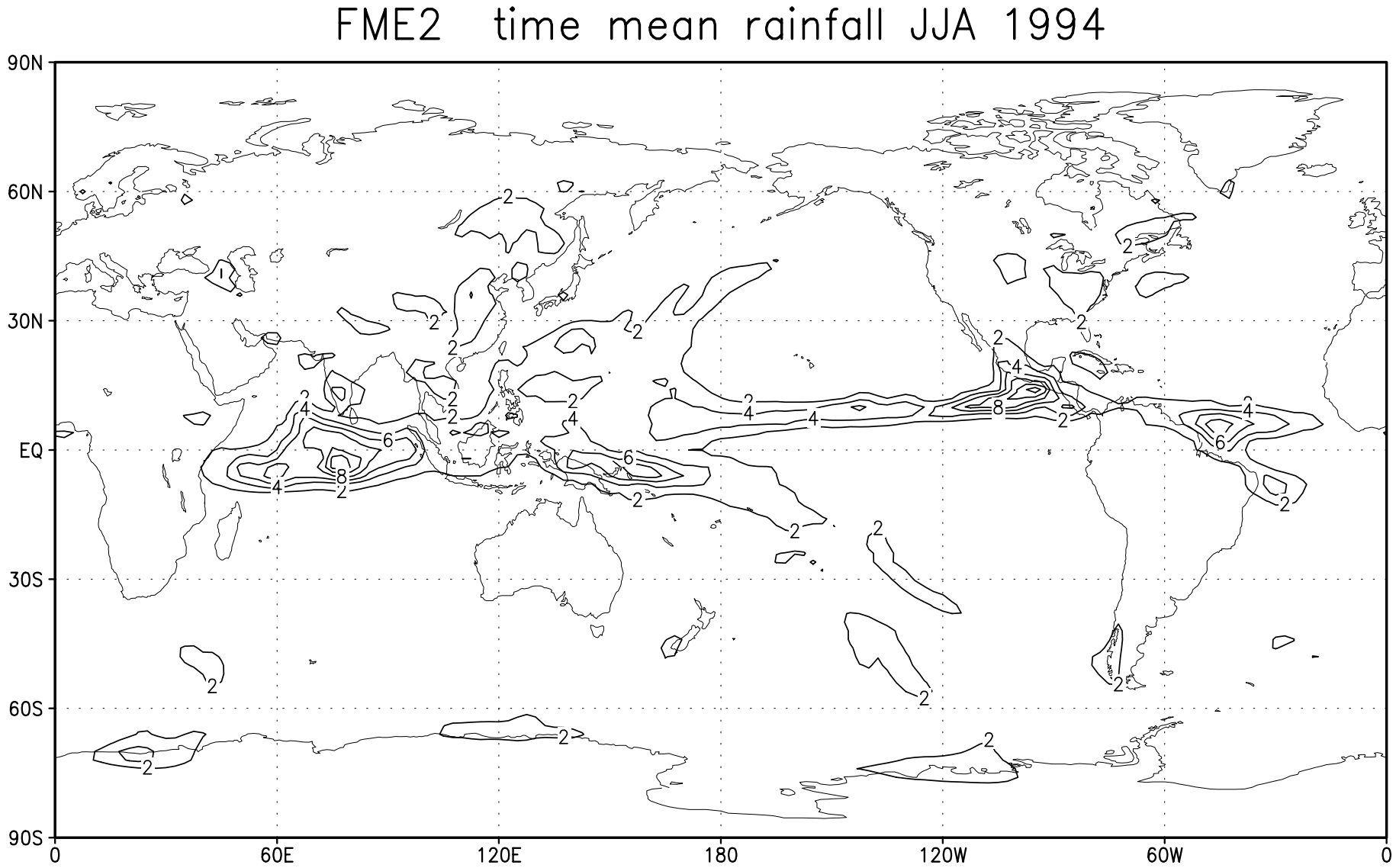

Fig. 5b June-July-August mean precipitation (mm/day) in 1994 for FME2.

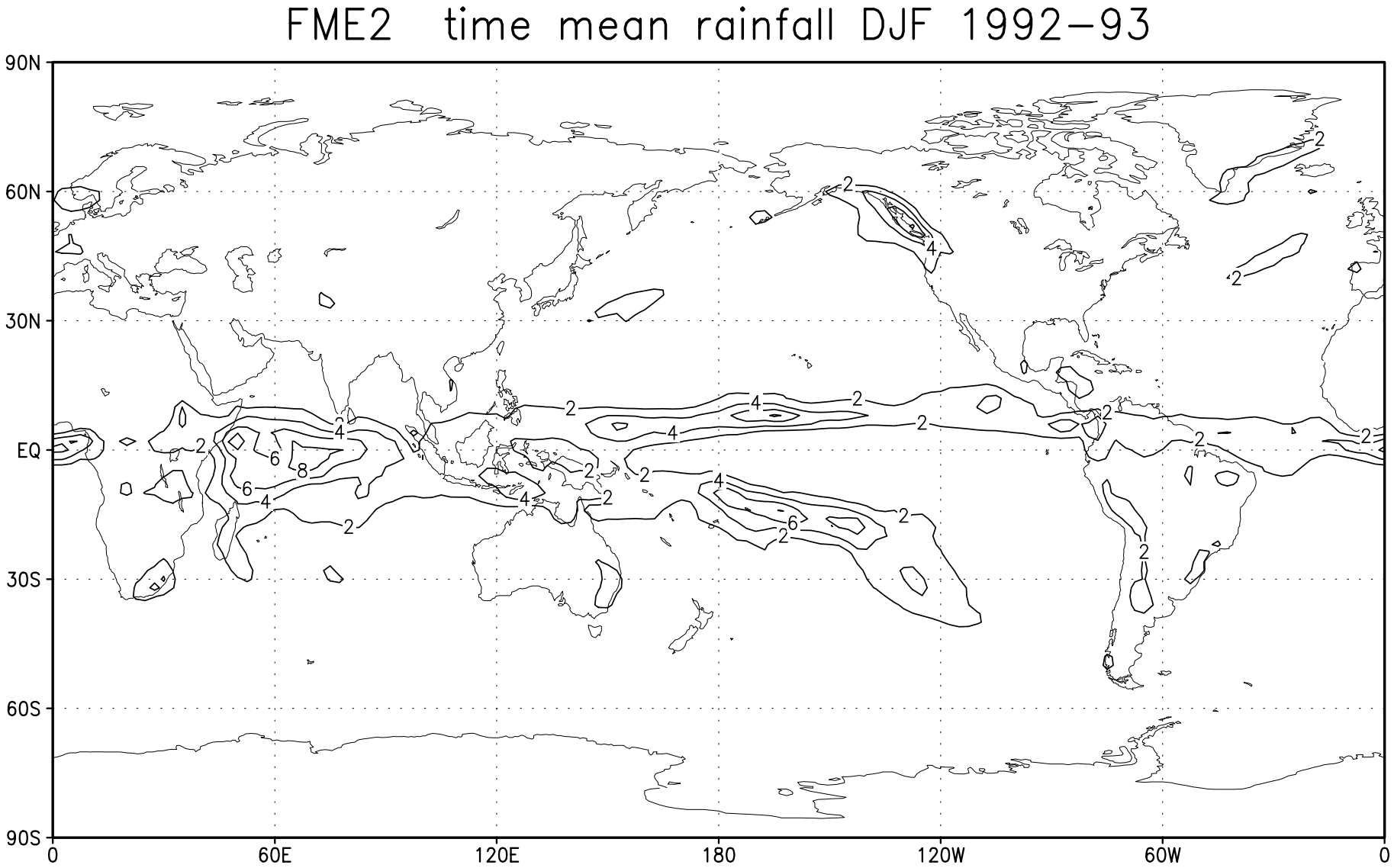

Fig. 5c December-January-February mean precipitation (mm/day) in 1992-93 for FME2.

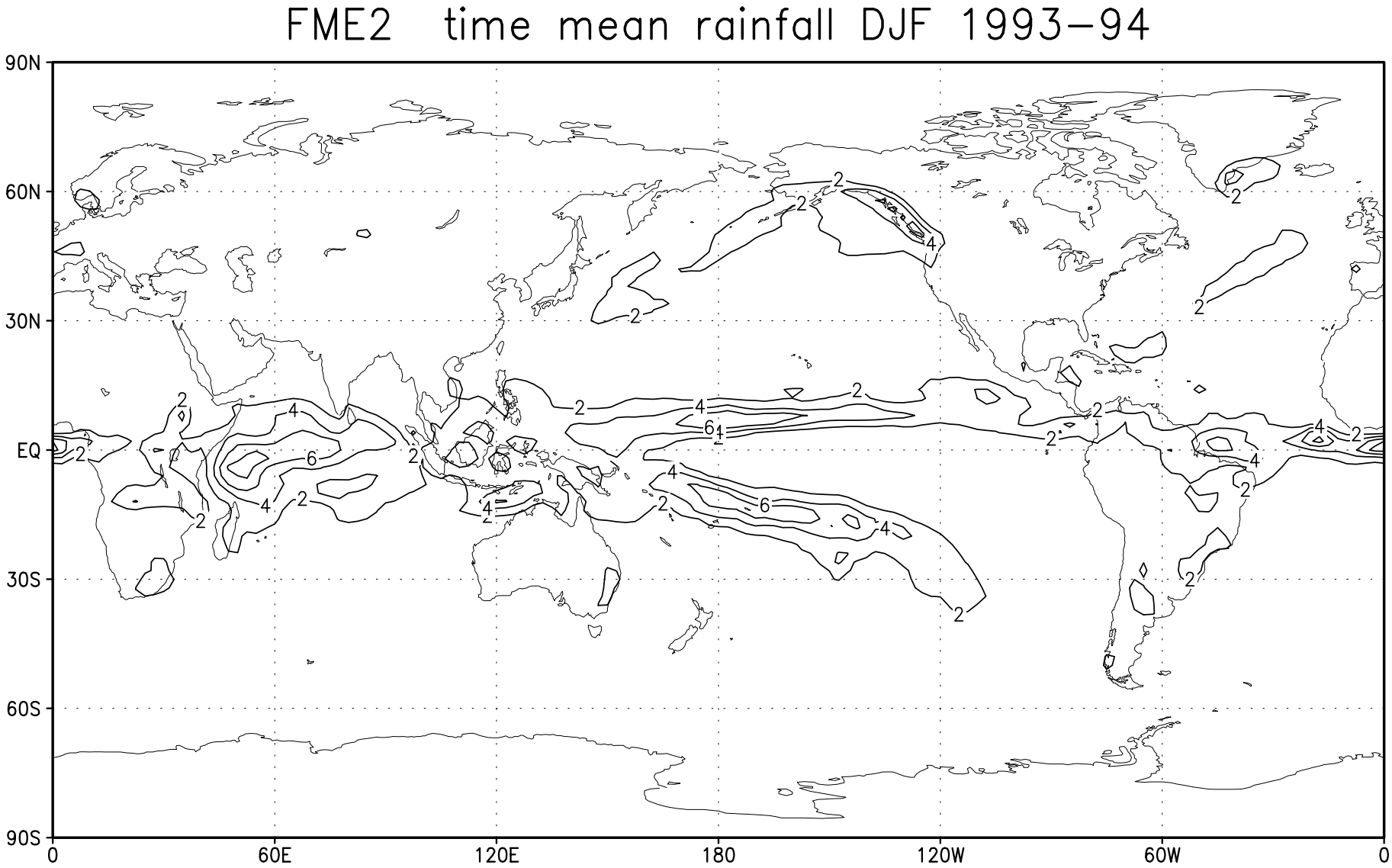

Fig. 5d December-January-February mean precipitation (mm/day) in 1993-94 for FME2.

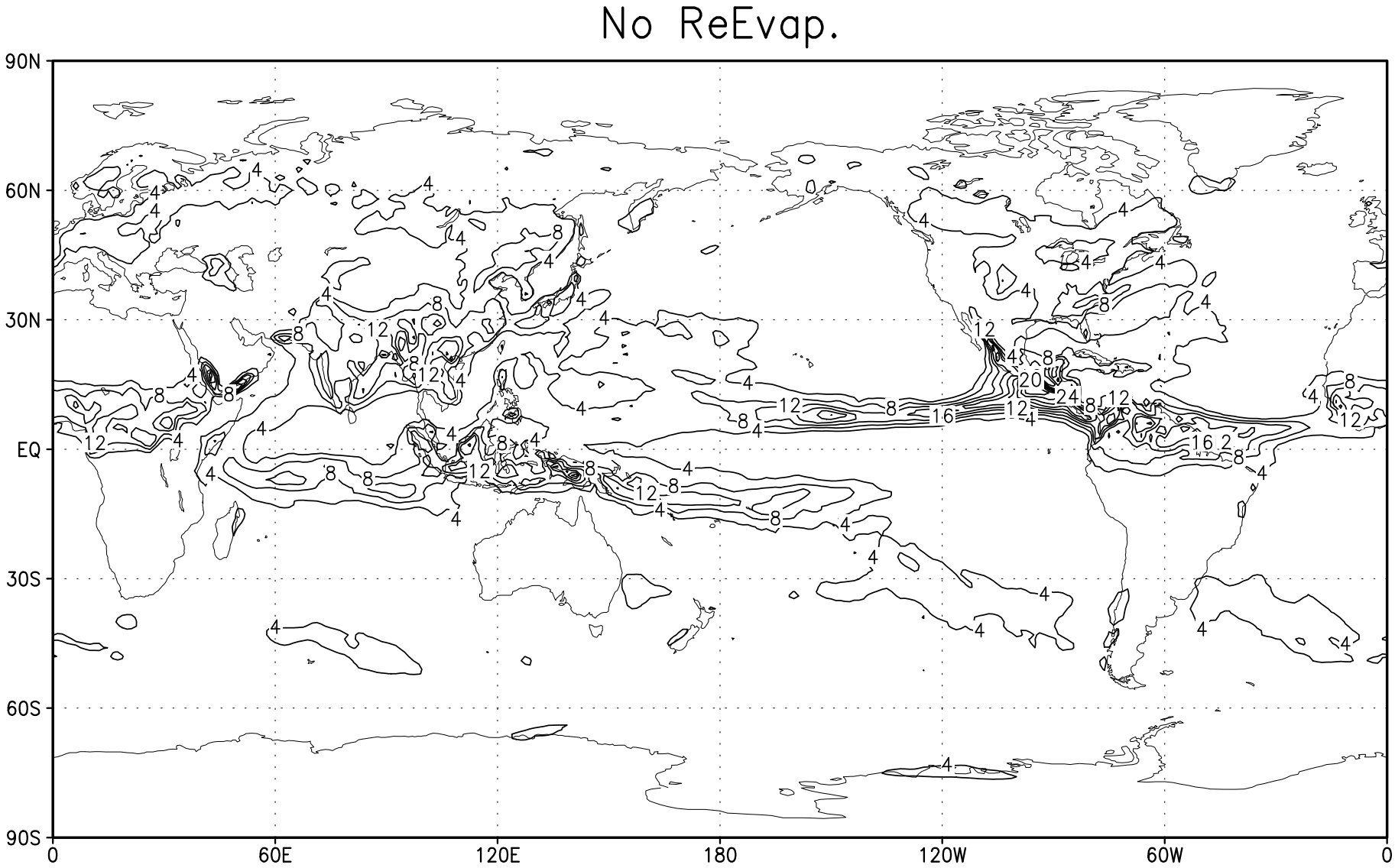

Fig. 6a June-July-August mean precipitation (mm/day) in 1995 without rain re-evaporation in an experiment with horizontal resolution doubled.

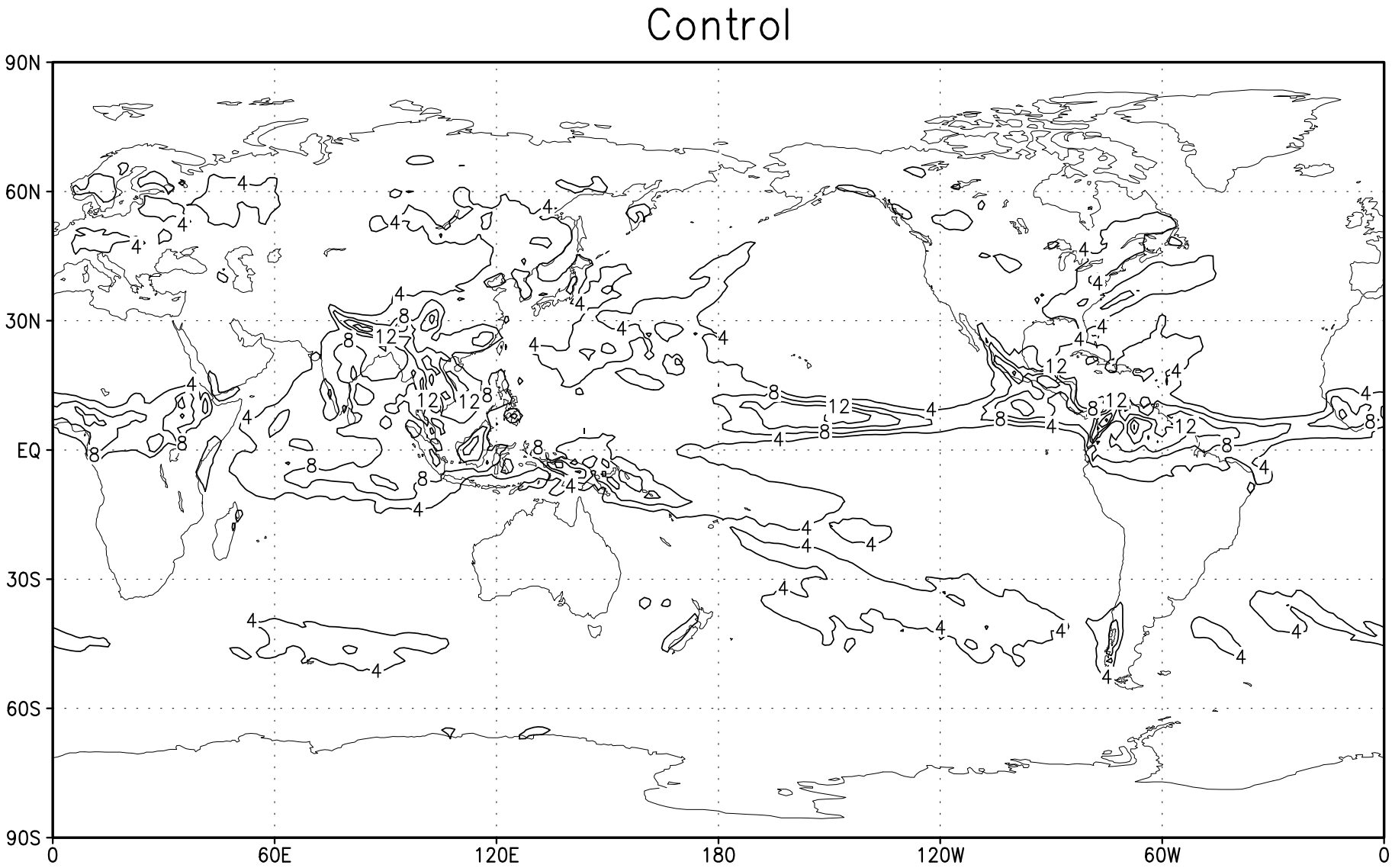

Fig. 6b June-July-August mean precipitation (mm/day) in 1995 with rain re-evaporation in an experiment with horizontal resolution doubled.

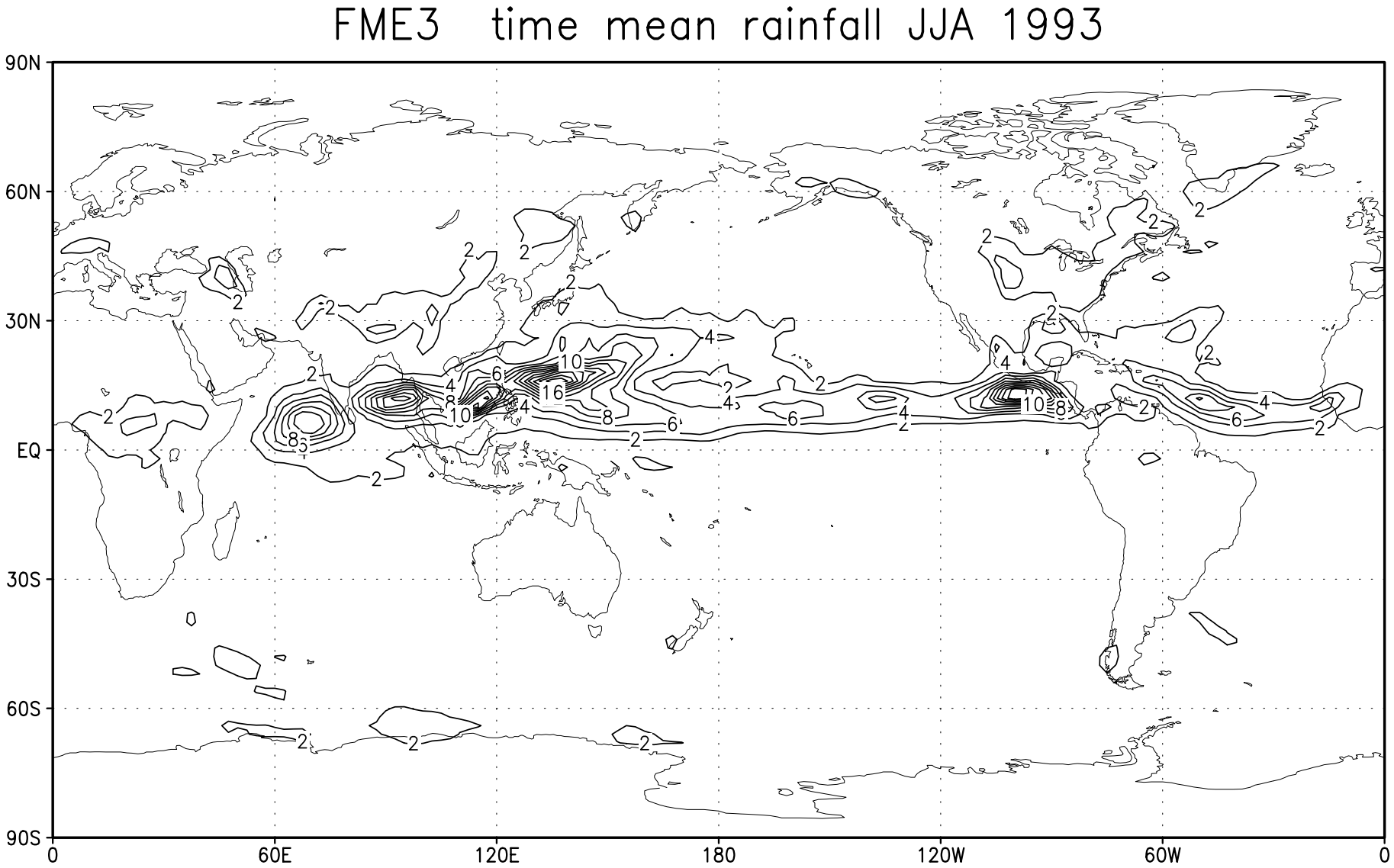

Fig. 7 June-July-August mean precipitation (mm/day) in 1993 for FME3.

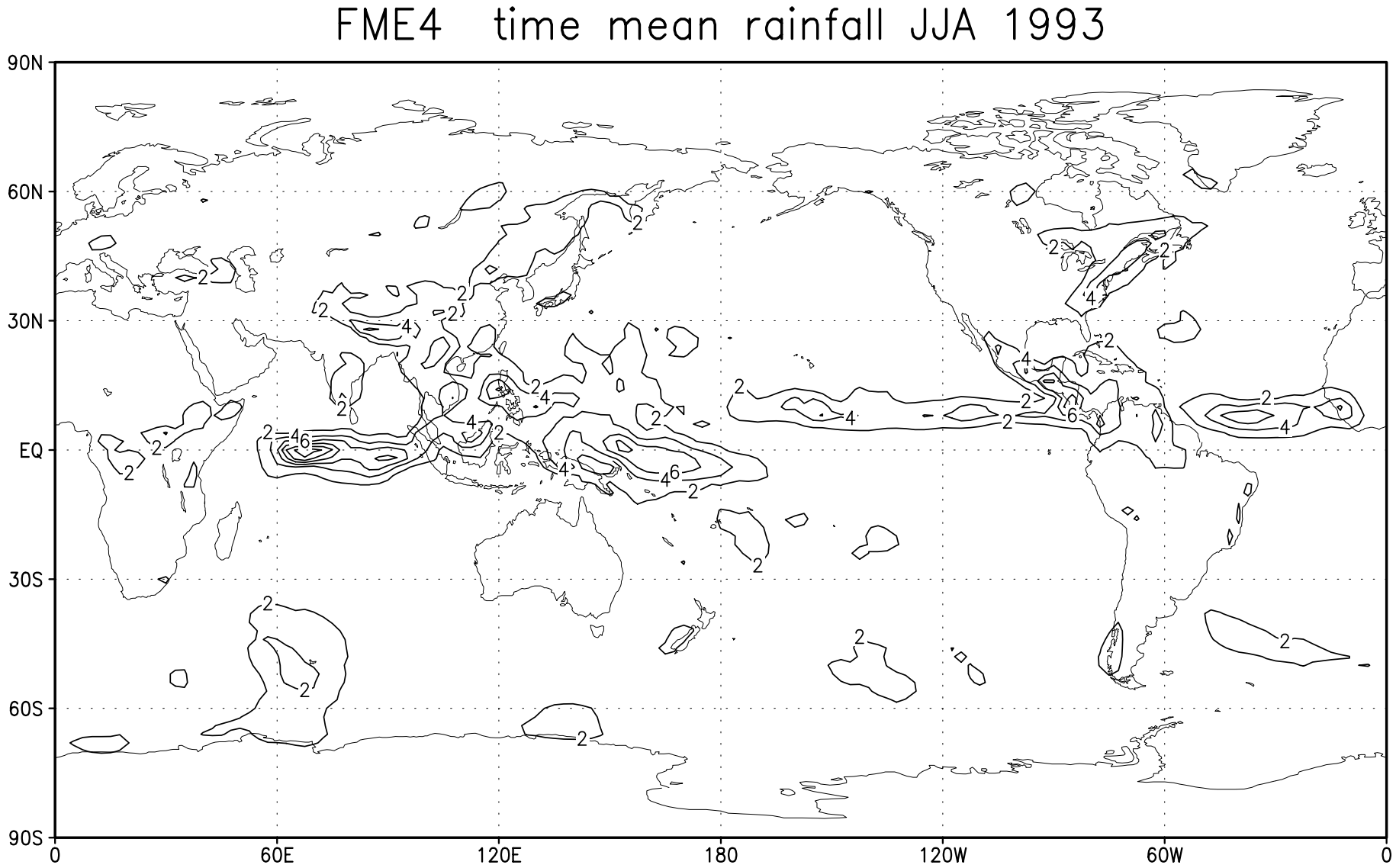

Fig. 8 June-July-August mean precipitation (mm/day) in 1993 for FME4.